

# QUARKS IN THE INSTANTON LIQUID-LIKE PICTURE OF THE QCD VACUUM \* \*\*

M. A. NOWAK

Institute of Physics, Jagellonian University  
Reymonta 4, 30-059 Cracow, Poland

*(Received July 4, 1991)*

We review a broad range of approaches to the problem of light quarks propagating through the instanton liquid-like vacuum of the Quantum Chromodynamics. Numerical and analytical techniques are presented.

PACS numbers: 12.38.Aw, 12.38.lg

## 1. Introduction

The understanding of the mechanism of spontaneous breakdown of chiral symmetry is one of the most fundamental problems in strong interaction physics. It is generally believed that this phenomenon stems from the complex non-perturbative character of the vacuum state [1].

There are three different approaches to understand the non-perturbative realm of the Quantum Chromodynamics. The first, most prominent and powerful is based on the Monte-Carlo simulation of a lattice-regularized version of QCD. This approach, for the first time has provided a method of quantitative studies of the non-perturbative aspects of QCD starting from the first principles. The second approach, known as the QCD sum rule approach [2], is based on Wilson operator product expansion of the correlation functions. The non-perturbative features of the QCD are introduced via expectation values of local gauge invariant operators. The third approach consists of a class of variational calculations based on the assumption that the perturbative vacuum is unstable in the infrared region. There

---

\* This paper is presented as the qualifying thesis for the habilitation at the Jagellonian University.

\*\* This work has been partially supported by the Polish Projects CPBP 01.03 and CPBP 01.09.

exist many examples of such calculations: the Savvidy-Copenhagen vacuum [3,4], the monopole vacuum [5], the glueball condensate vacuum [6]. The instanton liquid model of the vacuum also belongs to this class [7].

A distinguishing feature of the instantonic vacuum picture, which differentiates it from other models is the fact that instantons are so far the unique non-perturbative fluctuations of the gluon field found in QCD. Although so far it has been proven difficult to obtain *exact* dynamical statements concerning role of instantons in QCD, phenomenological analysis based on instantonic fluctuations successfully describes most of the features of the hadrons.

The primary motivation behind the instanton vacuum is to describe the bulk part of the nonperturbative gauge fluctuations at intermediate distance scales. There are strong indications from QCD sum rules that already at distance scales of about 0.1 fm the perturbative approach breaks down [8]. Instanton configurations constitute an important class of inhomogeneous gauge fluctuations that might be important at these distance scales. Unfortunately, inhomogeneous gauge configurations of this type are not sufficient to imply the confinement mechanism [9,10]. It is commonly thought that larger scale gauge fluctuations are necessary for disordering of the Wilson loop, and, in consequence, for the confinement. Since nothing is known about the nature and character of these gauge fluctuations, we will ignore them. Our hope is that the chiral symmetry breaking is primarily due to small and inhomogeneous gauge fluctuations and does not have to follow the general lore of confinement. The concept of dynamical mass generation put forward in [11,12] seems to imply that chiral symmetry restoration does not rule out dynamical confinement in the presence of light quarks.

Let us review briefly the history of main qualitative successes of the instanton vacuum picture in description of non-perturbative features of strong interaction physics. Instantons solve naturally the U(1) problem [13], they account for a non-perturbative gluon condensate [14] and lead to a crude mean field description of the spontaneous breakdown of chiral symmetry [15,16]. Unfortunately, the naive description of the instanton vacuum based on the dilute gas approximation is plagued with infrared divergences. In the dilute gas approximation instantons and anti-instantons tend to inflate, causing the partition function to diverge.

Diakonov and Petrov [17] have suggested that the infrared problem was inherent to the dilute gas approximation. The instanton-anti-instanton interactions in the vacuum produce overall repulsive interactions that stabilize the vacuum state. Variational calculations [17] have shown that instantons in the vacuum are in a liquid phase characterized by an interparticle separation of about 1 fm. The average size of the instantons in this phase is about 0.3 fm. In general, a random character of the instanton vacuum

leads to a delocalization of the 't Hooft's zero modes and implies the breakdown of chiral symmetry [18]. The variational analysis was carried out under the assumption that the collective coordinates of the pseudoparticles are distributed with a uniform weight. Recently, this assumption has been questioned by Shuryak [19,20] who has pointed out that there are strong induced fermion interactions in the vacuum that alter quantitatively the character of the vacuum state. Due to these interactions an "instantonic matter" may exist in gaseous, liquid or even in crystalline phase. Numerical simulations done by Shuryak [20,21], Nowak, Verbaarschot and Zahed [22] and recently by Shuryak and Verbaarschot [23] gave strong support to this multi-phase picture of the instantonic vacuum.

In this work we would like to concentrate on the effect of the light quarks propagating through the instantonic medium. We will review the broad range of approaches to the instantonic vacuum picture, both numerical and analytical. The presentation is based on a series of our papers published elsewhere [22,24–27]. In Chapter 2 we will remind some known properties of the instantons and we will summarize the main assumptions and approximations leading to the formulation of the instantonic vacuum. In Chapter 3 we will show how to simulate on computer the partition function of the topologically neutral ensemble of instantons and anti-instantons interacting with the light quarks and we will review some recent results in this field. We will also demonstrate, in some limiting cases, exact analytical crosschecks of the simulation. In Chapter 4 we will present the mean field approach to the chirally broken phase, in which fermion zero modes are entirely delocalized over the space. The resulting partition function will turn out to be equivalent to the partition function of constituent quarks interacting via 't Hooft vertices. Chapter 5 demonstrates how to incorporate effects of the temperature into the instanton description of the QCD vacuum with light quarks. By using the mean field technique, we will get the results for the constituent quark mass and condensates as a function of temperature and number of flavors. In Chapter 6, with the help of the coarse-graining technique, we will formulate the effective long-wavelength limit action for the instantonic vacuum and we will investigate some phenomenological consequences of these long wavelength excitations. Finally, Chapter 7 is devoted to the broad discussion of the advantages, disadvantages and future prospects of the instantonic vacuum picture for QCD. Some necessary conventions and technical details, as well as lengthy formulae, are presented in Appendices A and B.

## 2. Formulation of the Instanton Vacuum

### 2.a. Generalities on Instantons

Euclidean nonabelian gauge theories are characterized by topologically nontrivial gauge configurations (instantons). When the color gauge group is  $SU(2)$  an instanton of size  $\rho$  located at position  $z$  is given by

$$A_\mu = \frac{1}{2i} U (\tau_\mu^- \tau_\nu^+ - \tau_\nu^- \tau_\mu^+) U^\dagger \Pi \partial_\nu \Pi^{-1}, \quad (2.1)$$

where  $\tau_\mu^\pm = (\vec{\tau}, \pm i1)$  and  $U$  is a global  $SU(2)$  matrix and  $\Pi$  is given by

$$\Pi = 1 + \frac{\rho^2}{(x - z)^2 + \rho^2}. \quad (2.2)$$

The configuration (2.1) has the structure of a hedgehog in color and spin space. Anti-instantons are obtained from (2.1) by the transformation ( $\tau^\pm \rightarrow \tau^\mp$ ). For larger color groups, instanton configurations are obtained through various embeddings of the configurations (2.1). The gauge configuration (2.1) carries a unit topological charge,

$$\theta = \frac{1}{32\pi^2} \int d^4x \operatorname{Tr}(\epsilon_{\mu\nu\alpha\beta} F_{\mu\nu} F_{\alpha\beta}) = 1. \quad (2.3)$$

and saturates the BPST bound [28]. From the Atiyah–Singer index theorem it follows that the Dirac operator in the classical background (2.1) has a normalizable zero mode. It is given by

$$\phi_{\alpha\nu}^R = \frac{1}{2\sqrt{2}\pi\rho} \Pi^{\frac{1}{2}} \left[ \not{\partial} \left( \frac{\Phi}{\Pi} \right) \right]_{\nu\rho} \Omega_{\rho\beta} U_{\alpha\beta}, \quad (2.4)$$

where  $\Phi = \Pi - 1$  and  $\Omega$  is a  $4 \times 4$  matrix with the lower  $2 \times 2$  block equal to  $i\tau_2$  and all other matrix elements equal to zero. The matrix  $\Omega$  acts as a projector onto states with a definite chirality. The zero mode in Eq. (2.4) is righthanded. The zero mode corresponding to an anti-instanton solution is obtained from Eq. (2.4) by interchanging the  $2 \times 2$ -blocks on the diagonal of the matrix  $\Omega$ . It is obvious that this zero mode is left-handed. It will be denoted by  $\phi_{\alpha\nu}^L$ . The spectrum of the Dirac operator corresponding to an instanton is characterized by a gap of about  $\rho^{-1}$  between the zero energy state and the continuum of the scattering states. More details on instantons can be found in the excellent books by Rajaraman [29] and Polyakov [30].

### 2.b. Instantonic vacuum

Before we tackle the many-body instanton problem we first study the much simpler problem of a single instanton and a single anti-instanton. This configuration has a trivial topology. In the chiral limit it does not exhibit rigorous zero modes. To illustrate this we consider a gauge field configuration given by the linear superposition of an instanton and an anti-instanton. When the relative distance  $R$  between the pseudoparticles is finite, the zero modes start to overlap. More specifically, when we maintain a linear superposition of an instanton and an anti-instanton<sup>1</sup>, the eigenfunctions of the Dirac equation are given by  $\phi_{\pm} = (\phi^R \pm \phi^L)/\sqrt{2}$ . The corresponding energies are split about 0 by a gap of

$$\Delta = 2 \int \phi_R^\dagger i \not{\partial} \phi_L = 2D. \quad (2.5)$$

The overlap matrix  $D$  can be calculated explicitly (*cf.* Appendix A). Note that the overlap matrix is proportional to the cosine of a suitably defined relative orientation angle [31] between the instanton and the anti-instanton. The overlap is maximized for relative orientations of 0 and  $\pi$  (this resembles a dipole-dipole interaction). For asymptotically large values of  $R$  we find  $D \rightarrow R^{-3}$ . The dependence is the same as one found in the propagator of a noninteracting massless quark. For a small interparticle distance we obtain the dependence  $D \rightarrow R$ .

In the instanton model of the vacuum the QCD ground state is described by a statistical ensemble of  $N_+$  instantons and  $N_-$  anti-instantons in an Euclidean volume  $V_4$  with a partition function determined by the gauge field action [15,32,33]. To insure topological neutrality we require that the expectation value  $\langle N_+ - N_- \rangle = 0$ . To account for the U(1) anomaly, however, the topological susceptibility should be nonvanishing, *i.e.*,  $\langle (N_+ - N_-)^2 \rangle \neq 0$ . This is achieved by the thermodynamic fluctuations which are nonvanishing in the thermodynamic limit  $N_{\pm} \rightarrow N/2$ ,  $N \rightarrow \infty$ ,  $V_4 \rightarrow \infty$  at a fixed pseudoparticle density  $N/V_4$ .

In order to achieve a more quantitative understanding of the vacuum state we will adopt the approach of Shuryak [20] to truncate the Hilbert space of the fermions to the space of zero modes. This approximation is justified for the long wavelength properties of the vacuum (scales  $> 0.3$  fm). The reason is that the spectrum of the Dirac operator in the field of an instanton is characterized by a gap of about  $\rho^{-1} \sim 600$  MeV between the zero energy state and the continuum of scattering states. For a topologically neutral system of  $N = N_+ + N_-$  of pseudoparticles interacting with quarks occurring in  $N_f$  flavors it is given by [20]

---

<sup>1</sup> This assumption is justified by the simulation, see Chapter 3.

$$Z = \frac{1}{N_+!N_-!} \int \prod_I^N d\Omega_I d(\rho_I) \exp(-\beta(\rho)u_{\text{int}}) \prod_{i=1}^{N_t} \det(-i\gamma_\mu \nabla_\mu(A) - im_i), \quad (2.6)$$

In the above formula  $\Omega_I = \{z_I^\mu, \rho_I, U_I\}$  denotes the set of  $4N_c$  collective variables corresponding to each of the pseudoparticles. For each pseudoparticle we integrate over its position  $z^\mu$ , size  $\rho$  and  $4N_c - 5$  color variables corresponding to the relevant coset space  $SU(N_c)/[SU(N_c - 2) \times U(1)]$ . For the spatial variables, the integration measure is uniform inside the box defined by the periodic boundary conditions. The integration over the  $SU(N_c)$  variables is performed with the Haar measure (the normalization factor takes care of the coset structure). We do not need to integrate over the orientations of the pseudoparticles because instantons are hedgehog-like configurations in color and spin. The spatial directions are therefore “locked” by the color directions. The size distribution  $d(\rho)$  is given by [13]

$$d(\rho) = C\rho^{-5} (8\pi^2 g^2)^{2N_c} (M\rho)^{23N_t} \exp(-\beta(\rho)), \quad (2.7)$$

where  $\beta$  is the one-loop Gell-Mann Low function evaluated at a scale that is of the order of the size  $\rho$  of the instantons

$$\beta(\rho) = -b \ln(\rho\Lambda), \quad b = \frac{11}{3}N_c - \frac{2}{3}N_t, \quad (2.8)$$

and  $C = 4.60 \exp(-1.68N_c)/(\pi^2(N_c - 1)!(N_c - 2)!)$ .  $\Lambda$  is the ultraviolet cut-off in the Pauli-Villars scheme, and  $M$  is a renormalization mass. In deriving (2.6) it was assumed that the classical gauge field is a linear superposition of single instanton and anti-instanton field configurations

$$A_\mu(x) = \sum_I^{N_+} A_\mu^I(x) + \sum_I^{N_-} A_\mu^I(x). \quad (2.9)$$

The two-body interaction term  $u_{\text{int}}$  depends on the ansatz form. It was explicitly demonstrated for a couple of ansätze (“sum” ansatz (2.9) [17], “ratio” ansatz [31], “streamline” configuration [31]) that on average, the interaction term is repulsive [17,31,21,35]. It is a nice feature of the sum and ratio ansätze, that the repulsion is so strong at the classical level. This allows to approximate the quantum corrections to the interaction by the product of single-instanton quantum fluctuations. This assumption is justified if the system is rather dilute, a point to be checked *a posteriori*, as a consistency condition. In the present paper we will use the sum ansatz (2.9).

The fermion determinant in (2.6) involves the covariant derivative  $\nabla$  in the classical background of instantons and anti-instantons (pseudoparticles) (2.9), and a diagonal mass matrix  $m = \text{diag}(m_1, \dots, m_f)$  for  $N_f$  flavors. It can be factorized in a low momentum factor ( $\equiv \det_{\text{low}}$ ) and a high momentum factor ( $\equiv \det_{\text{high}}$ ). Both factors are regularized by a mass  $M$  and normalized by the non-interacting fermion determinant [18]. Specifically,

$$\det_{\text{high}} = \prod_{I,f} (M \rho_I)^{-\frac{3}{2}} 1.339 M_1 \rho_I, \quad M_1 \rho_I \ll 1, \quad (2.10)$$

where  $M_1$  is an arbitrary mass scale separating the low momentum components in the fermion determinant from the high momentum ones. The low momentum part of the fermion determinant can be saturated by fermionic zero modes [18]

$$\det_{\text{low}} = \prod_f \det(D + im_f K - im_f) / \det(D + im_f K - iM_1), \quad (2.11)$$

where the matrix elements of the hermitean matrices  $D$  and  $K$  are defined as follows

$$D_{IJ} = \int d^4x \phi_I^\dagger i \gamma_\mu \partial_\mu \phi_J, \quad (2.12)$$

$$K_{IJ} = \int d^4x \phi_I^\dagger \phi_J - \delta_{IJ}. \quad (2.13)$$

Their explicit form can be found in the Appendix A. For small current masses we may neglect  $K$ .  $\phi_I$  represents the fermionic zero mode in the field of one instanton or one anti-instanton. Of course, the full fermion determinant should be insensitive to the arbitrary mass  $M_1$ .

### 2.c. Chiral symmetry breaking order parameter

In the investigation of bulk properties of the vacuum state the quark and gluon condensates provide convenient order parameters. Full quark propagator in the instanton vacuum is given by

$$S(x, y, A) = \langle q(x) q^\dagger(y) \rangle = \langle (-i \nabla(A) - im)^{-1} \rangle, \quad (2.14)$$

where  $\langle \dots \rangle$  means

$$\langle \dots \rangle = \int \sum_{I=1}^N d\Omega_I d(\rho_I) e^{-\beta(\rho) u_{\text{int}}} \det(-i \gamma_\mu \nabla_\mu(A) - im) \dots \quad (2.15)$$

Spectral representation for  $S$  gives

$$S(x, y, A) = \sum \frac{\phi_n(x) \phi_n^\dagger(y)}{\lambda_n - im}, \quad (2.16)$$

where  $\phi_n$ ,  $\lambda_n$  are eigenvectors and eigenvalues of the Dirac equation  $-i\mathbb{V}(A)\phi_n(x) = \lambda_n\phi_n(x)$ . Using the relations between the formalism of the Euclidean and Minkowski spaces (cf. Appendix A) we can rewrite the quark condensate as a trace of the Euclidean propagator

$$\begin{aligned} \langle \bar{q}q \rangle_{\text{Mink}} &= \lim_{x \rightarrow y} i \langle q^\dagger(x) q(y) \rangle_{\text{E}} = i \text{Tr} \langle S(x, x, A) \rangle \\ &= i \text{Tr} \langle (i\mathbb{V}(A) - im)^{-1} \rangle = i \frac{1}{V_4} \int d\lambda \frac{\bar{\nu}(\lambda)}{\lambda - im}. \end{aligned} \quad (2.17)$$

where, in the last equation, we have introduced integration over the spectral density  $\bar{\nu}$  instead summing the eigenvalues. In the chiral limit ( $m \rightarrow 0^+$ ) Dirac operator  $\mathbb{V}$  anticommutes with  $\gamma_5$ , so the eigenvalues come in pairs  $(\lambda, -\lambda)$  and spectral function is symmetric. From the Dirac distribution formula

$$\frac{1}{\lambda \pm im} = P\left(\frac{1}{\lambda}\right) \mp i\pi\delta(\lambda) \quad (m \rightarrow 0^+) \quad (2.18)$$

we obtain

$$\langle \bar{q}q \rangle = -\frac{\pi}{V_4} \bar{\nu}(0). \quad (2.19)$$

The above formula states that the eigenvalue density of the Dirac operator at zero energy plays the role of an order parameter of the spontaneous breakdown of the chiral symmetry. In the next chapter we will see that when instantons form a gas phase of finite clusters,  $\bar{\nu}(\lambda)$  vanishes for  $\lambda = 0$ . Therefore  $\langle \bar{q}q \rangle = 0$  and, consequently, the vacuum is in the chirally symmetric state. However, in the liquid phase, instantons will form in general an amorphous, infinite network, leading to the entire delocalization of the zero modes and therefore to the fermion condensate.

### 3. Stochastic computer simulation

The stochastic simulation of the partition function provides the best *albeit* practically nontrivial way of getting information coming from the QCD vacuum in the instanton liquid model. Instead of simulation of the grand canonical ensemble, it is more pedagogical (and more easy) to study the partition function for zero temperature, at several densities (even unphysical), treating them as an external parameter. Even in this case the simulation of the partition function (2.6) is still a serious computational task, since



one has to perform simulation over  $4N_c N$  collective coordinates [36,31,21]. One can simplify the task by fixing the radius of the instantons on the basis of the quenched approximation. In such case the quantum effects do not depend on the instanton size. Such an approach was adopted by Shuryak [31] and by Nowak, Verbaarschot and Zahed [22]. Recently, high statistics, self-consistent numerical study of the instanton vacuum was completed by Shuryak and Verbaarschot [23]. The size of the instanton was determined by the dynamics of the partition function. Generally, most of the qualitative features of the vacuum, observed in earlier simulations, were confirmed. We will concentrate now on these features, postponing the discussion of some novel and unexpected results from [23] to the main part of this chapter.

In studying the partition function (2.6) the methods of statistical physics can be used extensively. One can either adopt standard Metropolis algorithm (as done in [23]) or, as in recent lattice QCD calculations, one can use the Langevin equation technique to get the equilibrium distribution. In the latter case (adopted by [22]), the evolution equation is given by

$$\partial_\tau \zeta_i = -\partial_{\zeta_i} W + \eta(\tau), \quad (3.1)$$

where  $\zeta_i$  is a collective coordinate and the action  $W$  is given by

$$W = \sum_{i=1}^{N_f} \text{Tr} \ln(m_i^2 + D^\dagger D) \quad (3.2)$$

and  $\eta$  represents a gaussian white noise with zero mean correlated to a Dirac delta

$$\overline{\eta(\tau)\eta(\tau')} = 2\delta(\tau - \tau'). \quad (3.3)$$

The overlap matrix  $D$  has been defined in Eq. (2.12). Since the coordinates of the instantons are Euclidean the Langevin equation (3.1) describes the motion of particles in a  $(4 + 1)$ -dimensional space in contact with a heat bath of unit temperature. The action  $W$  plays the role of a Hamiltonian. Elementary statistical physics suggests that the equilibrium distribution for the collective coordinates is  $\exp(-W)$ . Since our aim here is to present the physics of the chiral symmetry breaking and not the detailed numerology, we refer for details to the original paper [22].

To visualize the physics of the chiral symmetry breaking we draw an analogy with the statistical physics of the order-disorder phenomena [37]. We may imagine pseudoparticles as some atoms of two different kinds (instantons and anti-instantons), whereas the lowest atomic levels would correspond to the zero-modes of the Dirac equation in the field of the pseudoparticle. In the dilute system, quark wave functions (zero-modes) are well localized. However, in the case when the infinite cluster of pseudoparticles

(connected by the nearest neighbor overlap integrals  $D$ ) covers the entire space, zero modes become completely delocalized. Finding the probability of forming such an infinite cluster can be phrased as a kind of the percolation problem. Other analogies to order-disorder physics may be drawn as well [37]: *e.g.* the Anderson delocalization, maze conductivity, or metal-insulator Mott phase transition. The last analogy [36] is particularly striking — 't Hooft zero modes are analogs of the electron states at the edge of the Fermi surface and the appearance of the conductivity in solid becomes an analog of the chiral condensation in the vacuum.

It is intuitively obvious that the answer to these problems would depend on a density of pseudoparticles and on the number of “bonds” providing the overlaps  $D$ , *i.e.*, on the number of flavors. We strengthen this intuitive feeling by the following observation. Let consider a finite cluster ( $n$ ) of pseudoparticles in the dilute limit. Typically, this cluster will contribute a factor in the partition function of the form

$$\int \prod_{i=1}^n dz_i d\bar{z}_i \text{Tr}(D^\dagger D)^{nN_t} \sim V_4 R^{n(8-6N_t)-4}, \quad (3.4)$$

where  $R$  is a typical distance between neighboring instantons and an anti-instantons. For three flavors, large size clusters are suppressed, whereas for one flavor contributions from clusters of all possible sizes remain important. We see a quantitative difference between these two cases. For three flavors terms consisting of factors of two-cycles ( $n = 1$ ) are the dominant contribution in the dilute limit. This corresponds to the phase in which instantons and anti-instantons are forming the smallest possible cluster — the molecule, discussed in Chapter 2. This gaseous phase of small clusters, depicted schematically on Fig. 1a, we call a molecular phase.

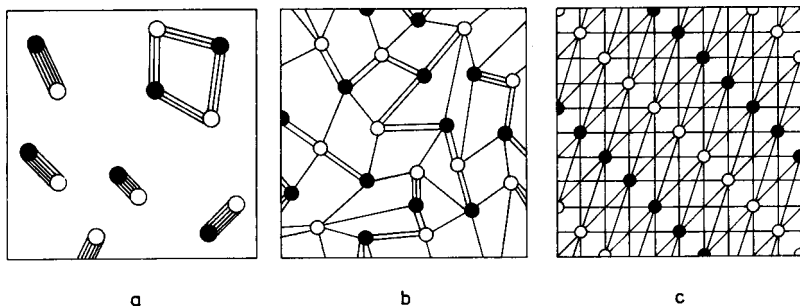


Fig. 1. Three phases of the instantonic “matter”. White and black circles represent instantons and anti-instantons, straight lines denote zero-mode “bonds”. a — molecular phase, b — liquid phase, c — crystalline phase - picture represents the projection of the four-dimensional *fcc* lattice.

The spectrum of the Dirac equation in this case resembles the inverted two-humped potential and vanishes for eigenvalues equal to zero. So in the molecular phase the chiral symmetry is unbroken. In the liquid phase (depicted schematically at Fig. 1b), pseudoparticles form an infinite, amorphous polymer. Due to a random character of the position and color distribution of the instantons in such a medium, the spectrum of this phase may lead to the breakdown of the chiral symmetry. We demonstrate this phenomenon explicitly in the limit  $N_c \rightarrow \infty$ . In this limit (*cf.* note at the end of Appendix B) the overlaps  $D_{IJ}$  are statistically independent, and the ensemble of the matrices  $D$  forms a Gaussian orthogonal ensemble. In this case, the spectrum  $\bar{\nu}(\lambda)$  of the eigenvalues of the overlap matrix  $D$  is known and is given by the semicircular formula of Wigner

$$\bar{\nu}(\lambda) = \frac{N}{\pi\kappa} \left(1 - \frac{\lambda^2}{4\kappa^2}\right)^{\frac{1}{2}}, \quad (3.5)$$

where the variance  $\kappa$  of the eigenvalues determines at  $\lambda = 0$  the value of the condensate. The chiral symmetry is spontaneously broken in this phase.

The above proof depends crucially on the limit  $N_c \rightarrow \infty$ . In practical calculations,  $N_c = 2$  or, more realistically<sup>2</sup>,  $N_c = 3$ , and only the numerical simulation can tell if the system is in the chirally broken or unbroken state. The nature of the phase transition is best illustrated by the eigenvalue density of the Dirac operator. Figure 2 shows spectral densities obtained during the Langevin simulation performed by Nowak, Verbaarschot and Zahed [22]. Figures a, b, c correspond to the low, physical and high density of instantons, respectively.

For the values of the densities and the masses we refer to the captions for the figures. For realistic quark masses and for physical density of the instantons the value of condensate is equal to  $|\langle \bar{u}u \rangle| = (220 \text{ MeV})^3$ .

The peak near zero at low density is the artefact of the process of dissociation of the molecules during the simulation and should be disregarded. An extrapolation of the slope leads to the vanishing spectral density  $\bar{\nu}(\lambda)$  in the case a and suggests the nonvanishing condensate in the cases b and c. The dip at zero resembles a finite size effect. Recent, high statistics simulation done by Shuryak and Verbaarschot [23] show how careful one should be when analyzing this dip. Their results demonstrate, that there is a qualitative difference in the nature of the dip between the  $N_f = 2$  and  $N_f = 3$  cases. In the case of the  $N_f = 2$ , the dip is indeed a finite size effect, and an extrapolation described above is correct, yielding the chiral condensate. However, in the case of three *massless* flavors, the dip is the genuine feature of the spectrum, even for physical densities. Moreover, at large densities the

---

<sup>2</sup> The qualitative features of the vacuum are similar in these two cases.

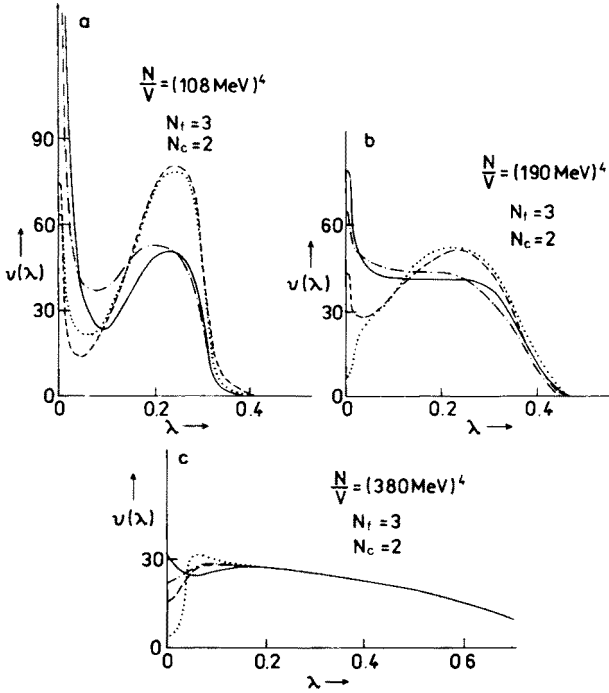


Fig. 2. The eigenvalue density  $\bar{\nu}(\lambda)$  as a function of  $\lambda$  for an instanton density: a —  $32/14^4 \rho^{-4} = (108 \text{ MeV})^4$ , b —  $32/8^4 \rho^{-4} = (190 \text{ MeV})^4$ , c —  $32/4^4 \rho^{-4} = (380 \text{ MeV})^4$ . The dotted line, the dashed line, the dashed-dotted line and the full line represent results with  $u$ -,  $d$ -,  $s$ -quark masses equal to  $(0, 0, 0)$  MeV,  $(12, 12, 12)$  MeV,  $(12, 12, 180)$  MeV and  $(30, 30, 30)$  MeV, in this order.

system seems to crystallize, realizing the scenario depicted schematically in Fig. 1c. The reason of the difference between  $N_f = 2$  and  $N_f = 3$  cases is so far unknown. Some speculation on this issue are presented in Chapter 7. We would like to stress, that the simulation for physical density in case of physical quarks masses equal to  $(0.05\Lambda, 0.05\Lambda, 0.1\Lambda)$  shows that the dip is the finite size effect and the chiral symmetry is of course broken. The results of the condensates are in reasonable agreement with phenomenology, *e.g.*,  $|\langle \bar{u}u \rangle| = (1.21 \pm 0.03)\Lambda^3$ ,  $|\langle \bar{s}s \rangle| = (0.73 \pm 0.01)\Lambda^3$  and the ratio of the strange quark condensate to the up quark condensate is 0.6 [23].

A convenient way to study the induced fermionic correlators is to look at so-called determinantal mass, defined as

$$m_\Delta = \left\langle \prod_{i=1}^{N_f} \left( \det(m_i^2 + D^\dagger D) \right)^{\frac{1}{N_f N}} \right\rangle. \quad (3.6)$$

In Fig. 3 and Fig. 4 we show the results for  $m_\Delta$  for one and three flavors.

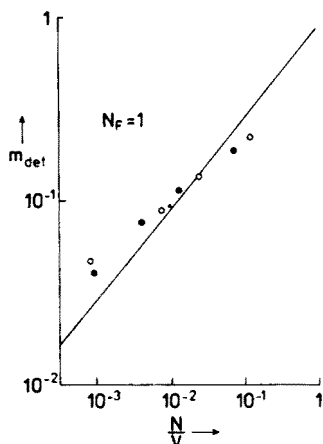


Fig. 3. The determinental mass  $m_{\text{det}}$  as a function of the instanton density  $N/V_4$  in the one flavor case with zero current quark masses. The full circles show results obtained by Shuryak [20] and the open circles are show results obtained by Nowak, Verbaarschot and Zahed [22]. The mean field result of Diakonov and Petrov [18] is given by the full line. The scale on both axis is logarithmic.

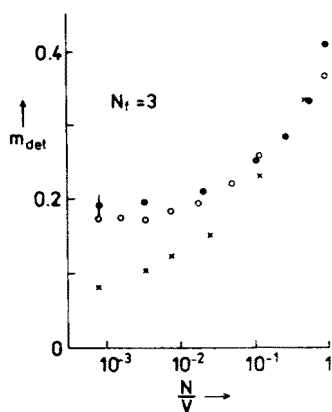


Fig. 4. The determinental mass  $m_{\text{det}}$  as a function of the instanton density  $N/V_4$  in the three flavor case. The full circles (results from Shuryak [20]) and the open circles (results from Nowak, Verbaarschot, Zahed [22]) show results obtained with zero current quark masses. The crosses represent our results for the case with current quark masses equal to (12, 12, 180) MeV.

Note, that in the case of one flavor the mean field description provides a fair description of the data. The solid line corresponds to

$$m_{\Delta} = \frac{m}{2} + \frac{1}{2}(m^2 + 4\kappa^2)^{\frac{1}{2}}, \quad (3.7)$$

where the semicircular variance defined by (3.5) was estimated in [18] as  $\kappa^2 = 6.06N/(V_4N_c)\rho^2$ . For the three flavors the fermionic correlations change the spectrum considerably.

Finally, we would like to discuss the two-point correlators in the instanton liquid model. Generally, the study of these correlators requires the knowledge of the eigenfunctions of matrix  $D$  as well as their eigenvalues. There exists however simple correlator,  $\partial_{m_s}\langle\bar{u}u\rangle$ , which can be expressed in terms of the eigenvalues of the matrix  $D$  only [22,25]. The interest in this quantity is not purely academic. In a naive quark model, this correlator can be related to the strange admixture in the nucleon state [38,25]

$$\langle N|\bar{s}s|N\rangle = M_N\partial_{m_s}\ln|\langle\bar{u}u\rangle|. \quad (3.8)$$

The partial derivative can be written in terms of the eigenvalues of the Dirac operator  $D$  as follows

$$\partial_{m_s}\langle\bar{u}u\rangle = \frac{1}{V_4}\int d\lambda d\lambda'\frac{\bar{\nu}_c(\lambda,\lambda')}{(\lambda+im)(\lambda'+im_s)}, \quad (3.9)$$

where  $\bar{\nu}_c(\lambda,\lambda')$  is a connected two-point correlation function defined by

$$\bar{\nu}_c(\lambda,\lambda') = \left\langle \sum_{i,j} \delta(\lambda - \lambda_i)\delta(\lambda' - \lambda_j) \right\rangle - \left\langle \sum_i \delta(\lambda - \lambda_i) \right\rangle \left\langle \sum_j \delta(\lambda' - \lambda_j) \right\rangle. \quad (3.10)$$

We should stress that the above two-point function carries a nontrivial mass dependence via the statistical average. Before we present numerical results we evaluate the derivative in two extreme cases. The first case is when the eigenvalues of  $D$  are uncorrelated and the second case is when the matrix elements of  $D$  are uncorrelated. The first case is a good approximation at low densities since the internal state of a single molecule does not depend on the internal state of the other molecules. At high densities we expect that the collective coordinates of the particles are distributed randomly. Then the overlap integrals are also distributed randomly. The corresponding eigenvalues will be highly correlated with correlation functions following the general formalism of random matrix theory [39,40].

When the eigenvalues are uncorrelated all terms in Eq. (3.10) with  $\lambda_i \neq \lambda_j$  cancel. From the diagonal terms we obtain

$$\partial_{m_s}\langle\bar{u}u\rangle = \frac{2m_s\langle\bar{u}u\rangle - 2m\langle\bar{s}s\rangle}{(m_s^2 - m^2)} - \frac{2V_4}{N}\langle\bar{s}s\rangle\langle\bar{u}u\rangle. \quad (3.11)$$

To leading order in  $\sqrt{\langle \lambda_i^2 \rangle} / m_s$  the terms that are inversely proportional to the density of instantons cancel. Notice that the connected two-point function corresponding to Eq. (3.11) is

$$\bar{\nu}_c(\lambda, \lambda') = \bar{\nu}(\lambda)\delta(\lambda - \lambda') - \frac{2}{N}\bar{\nu}(\lambda)\bar{\nu}(\lambda') \quad (3.12)$$

and satisfies the consistency condition  $\int d\lambda \bar{\nu}_c(\lambda, \lambda') = 0$ .

In the high-density limit the correlation function  $\bar{\nu}_c(\lambda, \lambda')$  is given by

$$\bar{\nu}_c(\lambda, \lambda') = \bar{\nu}(\lambda)\delta(\lambda - \lambda') - \bar{\nu}(\lambda)\bar{\nu}(\lambda')Y_2(r), \quad (3.13)$$

where  $Y_2(r)$  is Dyson's two-point cluster function for the gaussian orthogonal ensemble [41,42],

$$Y_2(r) = \frac{\sin^2 \pi r}{\pi^2 r^2} - \frac{\pi r \cos \pi r - \sin \pi r}{\pi r^2} \left( \int_0^r ds \frac{\sin \pi s}{\pi s} - \frac{1}{2} \frac{d}{dr} |r| \right) \quad (3.14)$$

and  $r$  is the distance between eigenvalues in units of the average level spacing ( $r = \int_{\lambda}^{\lambda'} \bar{\nu}(x) dx$ ). Asymptotically,  $Y_2(r)$  behaves as  $1/\pi^2 r^2$ . Its value at  $r = 0$  is equal to 1. The correlation function in Eq. (3.13) satisfies the consistency condition  $\int d\lambda \bar{\nu}_c(\lambda, \lambda') = 0$ . By using this property Eq. (3.9) can be rewritten as

$$\partial_{m_s} \langle \bar{u}u \rangle = \frac{1}{V_4} \int d\lambda d\lambda' \frac{2mm_s(\lambda^2 - \lambda'^2)^2 \bar{\nu}_{cl}(\lambda, \lambda')}{(\lambda^2 + m^2)(\lambda'^2 + m_s^2)(\lambda'^2 + m^2)(\lambda^2 + m_s^2)}, \quad (3.15)$$

where  $\bar{\nu}_{cl}$  is defined as  $\bar{\nu}_c(\lambda, \lambda') - \bar{\nu}(\lambda)\delta(\lambda - \lambda')$ . From Eq. (3.15) it is clear that the integrand can be approximated by the asymptotic result for  $Y_2(r)$ . The result is

$$\partial_{m_s} \langle \bar{u}u \rangle = \frac{-1}{V_4(m + m_s)^2}. \quad (3.16)$$

We conclude that at high instanton densities  $\partial_{m_s} \langle \bar{u}u \rangle$  vanishes in the thermodynamic limit.

Monte-Carlo results [22,25] for the correlation function  $\nu(\lambda, \lambda')$  are given in Fig. 5 and Fig. 6. These figures show whether the rather low realistic value of the instanton density is sufficient for the reproduction of the volume dependence given in (3.12).

The results for low density limit are given in Fig. 5. The values of the parameters are included in caption. The full line represents the two-point cluster function given in Eq. (3.14). For samples of  $N$  particles the two-point cluster function is  $-2/N$ . From this figure it is clear this result gives a fair description of the numerical data at low density and at zero masses.

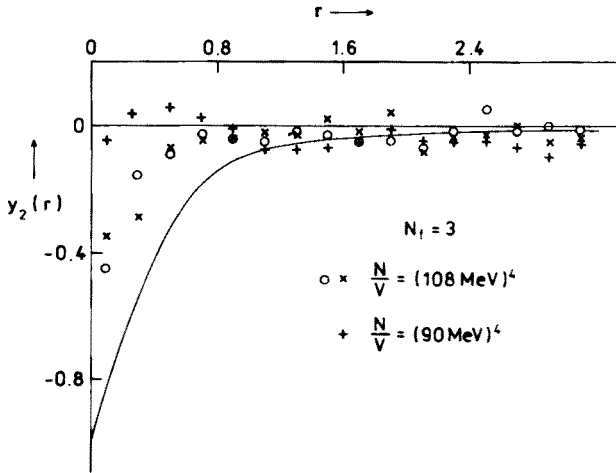


Fig. 5. The two-point function  $Y_2(r)$  at low instanton density. The quantity  $r$  is the distance between the eigenvalues in units of the average level spacing. The full line represents the random matrix result given in Eq. (3.14). The circles and the crosses show results for an instanton density of  $32/14^4 \rho^{-4} = (108 \text{ MeV})^4$  with 32 and 64 particles, respectively. The current quark masses are equal to (12, 12, 180) MeV. Results for massless quarks at a density of  $64/20^4 \rho^{-4} = (90 \text{ MeV})^4$  are given by the pluses.

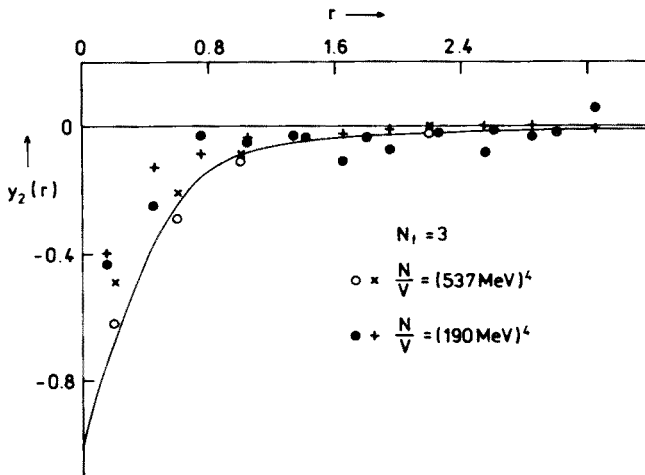


Fig. 6. The two-point function  $Y_2(r)$  at high instanton density. The circles and the crosses show results for an instanton density of  $0.5 \rho^{-4} = (537 \text{ MeV})^4$  with 32 and 64 particles, respectively. Results at the realistic density of  $32/8^4 \rho^{-4} = (190 \text{ MeV})^4$  are given by the full circles (32 particles) and the pluses (64 particles). The quark masses are equal to (12, 12, 180) MeV. For further explanation see the caption of Fig. 5.



For finite masses the chiral symmetry is broken. This results in the dissociation of the instanton molecules and gives rise to stronger correlations between the eigenvalues. Indeed, this is what is shown in this figure for the massive quarks. Results for a high and a realistic value of the instanton density are given in Fig. 6. The random matrix correlation function is close to the simulated data, in particular at the highest density. In view of these results we expect that the derivative  $\partial_m \ln |\langle \bar{u}u \rangle|$  is inversely proportional to the volume. These results show that the chiral condensate of the light quarks is very insensitive to the mass of the strange quark.

#### 4. Mean field approach to the instantonic vacuum

In so far our considerations of the fermionic degrees of freedom in the medium of instantons and anti-instantons have been exact to the extent that the fermionic Hilbert space is truncated to the space of the zero modes. We have indicated however, that this is a fair approximation for observables that vary slowly on the distance scales of about the size of the instanton. It was 't Hooft [13] who pointed out that at scales larger than the instanton size, the effects of a *single* instanton on the light quarks can be absorbed in terms of the effective *albeit* nonlocal interaction. An interesting question in this respect is whether one can derive in our framework an effective description in terms of long wavelength characteristics of the vacuum state, *i.e.*, some sort of an effective action. The answer to this question was proposed in [43,22,26]. In this chapter we will show how to extract an effective theory for the constituent quarks in the case of the instantonic liquid phase. In the following we will restrict ourselves to the case, when color orientations and positions of the instantons are distributed according to their invariant measure. This corresponds to a mean-field (or quenched) approximation, since we neglect in this way the correlations induced by the fermionic determinant. We stress that the simulated results discussed in the preceding chapter indicate the strong effect of these fermionic correlations for the case of two and more flavors. Therefore the analysis presented here provides only some qualitative insights and guidelines for the effective models in understanding the pattern of the chiral symmetry breakdown. Most arguments are given for a general value of  $N_c$ .

Consider the single particle propagator of a quark in a random medium of instantons and anti-instantons. In passing by an instanton, the quark can either scatter off or be trapped into the bound state. In the long wavelength limit one can assume the scattered waves to be free waves (without distortion). In this case, we may use the well known formalism of the scattering

on many-body centers:

$$S = S_0 + \sum_I (S_I - S_0) + \sum_{I \neq J} (S_I - S_0) S_0^{-1} (S_J - S_0) + \dots \quad (4.1)$$

where  $S_0$  is the free propagator and  $S_I$  is the propagator in the background of the single instanton  $I$ :

$$\begin{aligned} S_0 &= (-i\hat{D} - im)^{-1}, \\ S_I &= (-i\hat{D} - iA_I - im)^{-1}. \end{aligned} \quad (4.2)$$

Since the instanton fields are short ranged,  $S_I$  can be approximated by the sum of a free propagator and a nonperturbative contribution. At low energies the latter contribution is dominated by dilatational zero modes  $\phi_I$ , suggesting the following approximation for  $S_I$  [44,18]

$$S_I \sim S_0 + \frac{\phi_I \phi_I^\dagger}{-im}. \quad (4.3)$$

By using (4.3), the full propagator (4.1) can be rewritten as [18]

$$S = S_0 + \phi_I (D - im)_{IJ}^{-1} \phi_J^\dagger, \quad (4.4)$$

where  $D_{IJ}$  is the overlap matrix defined by (2.11).

Diakonov and Petrov [17] have shown that the interaction between instantons provides a Gaussian cutoff for the  $\rho$ -integration, leading to a strongly peaked distribution over the instanton size in (2.6). From their results it can be concluded that the variance of this distribution is inversely proportional to  $N_c$ . Thus, we will assume that the size integration can be performed by a lowest order cumulant expansion where the average size is determined by either the variational calculations or by the exact Monte-Carlo simulations.

Let us now investigate the many-body determinant  $\langle \det S^{-1} \rangle$  in the instanton liquid state where  $\langle \dots \rangle$  denotes the average over the collective coordinates. The low-momentum factor of the fermion determinant can be written as

$$\begin{aligned} \det_{\text{low}} &= \det S^{-1} / \det S_0^{-1} \\ &= \exp \left( - \text{Tr} \int_m^M \frac{i dm}{i\gamma_\mu \nabla_\mu + im} + \text{Tr} \int_m^M \frac{i dm}{i\gamma_\mu \partial_\mu + im} \right) \\ &= \exp \left( \int_m^M i dm \text{Tr}(S - S_0) \right) \end{aligned}$$

$$\begin{aligned}
 &= \exp \left( \int_m^M i \, dm \, \text{Tr} [\phi_I (D - im)^{-1}_{IJ} \phi_J] \right) \\
 &= \det(D - im) / \det(D - iM).
 \end{aligned} \tag{4.5}$$

In the above string of equalities we used the definition of  $D$ , formula (4.4) and we assumed that zero modes belonging to different instantons are orthogonal. Since the factor involving  $M$  cancels against the high momentum factor of fermion determinant, we will investigate the partition function defined as follows

$$Z = \det(-S_0^{-1}) \langle \det(D - im) \rangle. \tag{4.6}$$

To display the dynamical properties of the partition function we use a trick due to Ilgenfritz [45] to rewrite the determinants in Eq. (4.5) in terms of integrals over Grassmann variables (the explicit summation over pseudoparticles, Dirac, flavor and color indices is omitted in the exponent)

$$\begin{aligned}
 \det(-S_0^{-1}) &= \int d\psi d\psi^\dagger \exp \left( \int \psi^\dagger (i\partial_\mu \gamma_\mu + im) \psi \right), \\
 \det(D + im) &= \int d\chi d\chi^\dagger \exp \left( \chi^\dagger \left( \int \phi^\dagger i\partial_\mu \gamma_\mu \phi - im \right) \chi \right).
 \end{aligned} \tag{4.7}$$

For fixed values of  $\chi$  and  $\chi^\dagger$  a shift in the Grassmann variables  $\psi$  and  $\psi^\dagger$  by  $\psi \rightarrow \psi + i\phi\chi$ , and  $\psi^\dagger \rightarrow \psi^\dagger + i\chi^\dagger\phi^\dagger$  yields

$$\begin{aligned}
 \langle \det(-S^{-1}) \rangle &= \left\langle \int d\psi d\psi^\dagger \exp \left( - \int \psi^\dagger S_0^{-1} \psi \right) d\chi d\chi^\dagger (-i)^{-NN_f} \right. \\
 &\quad \times \exp \left( i\chi^\dagger \int \phi^\dagger S_0^{-1} \psi + \int i\psi^\dagger S_0^{-1} \phi \chi - im\chi^\dagger \chi \right) \Bigg\rangle.
 \end{aligned} \tag{4.8}$$

Using the chiral properties of the zero modes one can show that in the limit  $m \rightarrow 0$ ,  $\det S^{-1}$  is invariant under  $U_L(N_f) \times U_R(N_f)$  transformations of the fermion field  $\psi$ . Now we rewrite the sum over the instanton and anti-instanton indices  $I$  and flavor indices  $f$  in the exponent of (4.8) as a product over  $I$  and  $f$ . Due to the Grassmannian character of the variables only the zero and the first order terms of the Taylor expansion of the exponent are nonzero. Thus, the  $\chi_{I,f}^\dagger, \chi_{I,f}$ -integrals are Gaussian and can be evaluated in a straightforward way. The result is,

$$\begin{aligned}
 \langle \det(-S^{-1}) \rangle &= \int d\psi d\psi^\dagger \exp \left( - \int \psi^\dagger S_0^{-1} \psi \right) \\
 &\quad \times \left\langle \prod_{I,f} \left( i \int \psi^\dagger S_0^{-1} \phi_I \int \phi_I^\dagger S_0^{-1} \psi \right) \right\rangle.
 \end{aligned} \tag{4.9}$$

In order to obtain the last term of this equation, we have reversed the order of  $\psi$  and  $\psi^\dagger$ . By using the Grassmannian properties of the fermion fields, in this case Eq. (4.9) can be rewritten in terms of a determinant in flavor space as

$$\langle \det(-S^{-1}) \rangle = \int d\psi d\psi^\dagger \exp \left( - \int \psi^\dagger S_0^{-1} \psi \right) \times \prod_I \frac{1}{N_f!} \left\langle \det_{fg} \left( i \int \psi^\dagger f S_0^{-1} \phi_I \int \phi_I^\dagger S_0^{-1} \psi g \right) \right\rangle. \quad (4.10)$$

Since the zero modes have definite chirality, the determinantal factor in (4.10) breaks explicitly the  $U_A(1)$  symmetry and induces nonlocal interactions between fermions on the scale of the size of the instantons. At the mean-field level they also induce the spontaneous breakdown of chiral symmetry.

For reasons of simplicity, we will demonstrate here the calculation of this determinant for one flavor case. Then, we will present the results for  $N_f = 2, 3$ .

In the  $N_f = 1$  case, integration over the color group can be done easily with the help of formula (B.2) (cf. Appendix B). One obtains

$$Z = \int d\psi d\psi^\dagger \exp \left( \int d^4x \psi^\dagger i \not{\partial} \psi \right) \Theta_+^{N_+} \Theta_-^{N_-}, \quad (4.11)$$

where

$$\Theta_\pm = -\frac{1}{N_c V_4} \int \frac{d^4k}{(2\pi)^4} k^2 \varphi'^2(k) \psi_\alpha^\dagger(k) \gamma_\mp \psi_\alpha(k). \quad (4.12)$$

Here  $\varphi'$  is the Fourier transform of the 't Hooft zero modes [16,18] and  $\gamma_\pm = (1 \pm \gamma_5)/2$ . If we notice that the  $\Theta$  terms in (4.11) play the role of 'fugacities' in an otherwise conventional partition function, then  $Z$  can be analyzed using standard techniques from statistical mechanics. More specifically, with the help of the inverse Laplace transform

$$\Theta_\pm^{N_\pm} = \frac{N_\pm!}{2i\pi} \int_{\epsilon-i\infty}^{\epsilon+i\infty} d\beta_\pm \frac{1}{\beta_\pm^{N_\pm+1}} \exp(-\beta_\pm \Theta_\pm) \quad (4.13)$$

we can rewrite (4.12) in terms of only quark bilinears. Since the convergence of the integrals does not enter in the derivation of the mean field equations, we will omit the range of integrations from now on. The fermionic integrations can then be performed analytically. Up to constant factors we obtain

$$Z = \int d\beta_\pm \exp \left( - (N_+ + 1) \ln \beta_+ - (N_- + 1) \ln \beta_- \right) \times \exp \left( V_4 N_c \int \frac{d^4k}{(2\pi)^4} \text{Tr} \ln \left( \not{k} + i \gamma_\pm \frac{\varphi'^2(k) k^2 \beta_\mp}{N_c} \right) \right). \quad (4.14)$$

In order to stress that the saddle point approximation is exact in the thermodynamic limit we have transformed the variables  $\beta_{\pm} \rightarrow V_4 \beta_{\pm}$ . Note that due to the two-point 'vertex' generated by the instantons the fermion determinant in (4.14) contains a constituent mass term. In the thermodynamical limit ( $N_{\pm}$  and  $V_4 \rightarrow \infty$  with  $N/V_4$  finite) the integration in (4.14) can be performed by the saddle point method. For  $N_+ = N_- = N/2$  this leads to the following gap equation

$$\int \frac{d^4 k}{(2\pi)^4} \frac{M^2(k)}{k^2 + M^2(k)} = \frac{N}{4N_c V_4} \quad (4.15)$$

where

$$M(k) = \frac{\varphi'^2(k) k^2 \beta}{N_c}. \quad (4.16)$$

Since  $\beta_+ = \beta_-$  for  $N_+ = N_-$ , we have omitted the subscripts  $\pm$ . When we make the identification  $\varepsilon = \beta V_4 / N$  we obtain the gap equation derived by Dyakonov and Petrov [18]. Remember that in our case the pseudoparticle density  $N/V_4$  is proportional to the vacuum gluon condensate. Using the value of the gluon condensate suggested by the QCD sum rules ( $N/V_4 \sim (200 \text{ MeV})^4$ ), one obtains from Eq. (4.15) a constituent quark mass  $M(0)$  of about 345 MeV and a quark condensate of about  $(-250 \text{ MeV})^3$ .

Consider now the case of two and more flavors. In this case the partition function involves both quartic and sextic fermionic operators around the single instanton (anti-instanton). In other words, the instanton (anti-instanton) can trap  $N_f$  quarks (antiquarks) with different flavors. The group averaging is equivalent to the projection onto a color singlet and can be performed with the help of the relations (B.3) and (B.5) from Appendix B. Proceeding as for one flavor and using several Fierz identities, we obtain the following expression for the determinant in the partition function (4.10)

$$\begin{aligned} \frac{1}{2} \langle \det_{fg} \rangle_{N_f=2} &= \frac{1}{4(N_c^2 - 1)} k^4 \varphi'^4 \left( \left( 1 - \frac{1}{2N_c} \right) (\psi^\dagger \gamma_+ \tau^a \psi)^2 \right. \\ &\quad \left. + \frac{1}{8N_c} (\psi^\dagger \gamma_+ \tau^a \sigma_{\mu\nu} \psi)^2 \right) + (\gamma_5 \leftrightarrow -\gamma_5). \end{aligned} \quad (4.17)$$

Here,  $\psi$  is an isodoublet of the  $u$  and  $d$  quark fields, the 4-vector  $\tau^a$  has components  $(i1, \tau^i)$  with the  $\tau^i$ ,  $i = 1, 2, 3$  equal to the Pauli matrices acting in isospin space. We have used the convention  $\sigma_{\mu\nu} = \frac{1}{2}[\gamma_\mu, \gamma_\nu]$ . We recognize the expected 't Hooft interaction, but the interactions are smeared over the size of an instanton [43]. The case of three flavors is most complicated. The

effective sextic vertex for three flavors and for two or three colors<sup>3</sup> reads [22]

$$\begin{aligned}
 \frac{1}{3!} \langle \det_{fg} \rangle_{N_f=3} &= \int dR_{u,d,s}^3 \left( c_1 \mathcal{U} \mathcal{D} S - i c_4 f_{abc} \mathcal{U}_{\mu\nu}^a \mathcal{D}_{\nu\rho}^b S_{\rho\mu}^c \right. \\
 &\quad - \frac{N_c - 2}{N_c} c_3 d_{abc} \mathcal{U}^a \mathcal{D}^b S^c \\
 &\quad + c_2 \frac{N_c - 2}{N_c} (\mathcal{U} \mathcal{D}^a S^a + \mathcal{U}^a \mathcal{D}^a S + \mathcal{U}^a \mathcal{D} S^a) \\
 &\quad - \frac{1}{4} c_2 (\mathcal{U} \mathcal{D}_{\mu\nu}^a S_{\mu\nu}^a + \mathcal{U}_{\mu\nu}^a \mathcal{D}_{\mu\nu}^a S + \mathcal{U}_{\mu\nu}^a \mathcal{D} S_{\mu\nu}^a) \\
 &\quad \left. - \frac{1}{4} c_3 d_{abc} (\mathcal{U}^a \mathcal{D}_{\mu\nu}^b S_{\mu\nu}^c + \mathcal{U}_{\mu\nu}^a \mathcal{D}^b S_{\mu\nu}^c + \mathcal{U}_{\mu\nu}^a \mathcal{D}_{\mu\nu}^b S^c) \right) \\
 &\quad + (\gamma_5 \leftrightarrow -\gamma_5). \tag{4.18}
 \end{aligned}$$

We have introduced the notations

$$\mathcal{U} = u_a^\dagger(k_u) \gamma_+ u^a(q_u), \tag{4.18a}$$

$$\mathcal{D}^i = d_a^\dagger(k_d) \gamma_+ [\lambda^i]_b^a d^b(q_d), \tag{4.18b}$$

$$S_{\mu\nu}^i = s_a^\dagger(k_s) \gamma_+ [\lambda^i]_b^a \sigma_{\mu\nu} s^b(q_s). \tag{4.18c}$$

Other quantities appearing in Eq. (4.18) are defined by straightforward substitutions, *e.g.*,  $\mathcal{D} = \mathcal{U}(u \rightarrow d, k_u \rightarrow k_d, q_u \rightarrow q_d)$ . The measure is defined as

$$\begin{aligned}
 dR_{u_1, \dots, u_{N_f}}^{N_f} &= (2\pi)^4 \delta^{(4)} \left( \sum_{i=1}^{N_f} q_{u_i} - \sum_{i=1}^{N_f} k_{u_i} \right) \\
 &\quad \times \prod_{i=1}^{N_f} \frac{d^4 k_{u_i}}{(2\pi)^4} \frac{d^4 q_{u_i}}{(2\pi)^4} \varphi'(k_{u_i}) k_{u_i} \varphi'(q_{u_i}) q_{u_i}. \tag{4.19}
 \end{aligned}$$

and factors depending on  $N_c$  are defined by

$$\begin{aligned}
 c_1 &= \frac{1}{N_c^3}, & c_2 &= \frac{1}{4N_c(N_c^2 - 1)}, \\
 c_3 &= \frac{N_c}{8(N_c^2 - 1)(N_c^2 - 4)} \sqrt{\frac{N_c - 2}{3N_c}}, & c_4 &= \frac{1}{32N_c(N_c^2 - 1)}. \tag{4.20}
 \end{aligned}$$

Apart from the smearing effects, the terms in (4.18) agree exactly with the terms derived by Shifman, Vainshtein and Zakharov [46] using the operator product expansion. By explicit calculation, using extensively color

<sup>3</sup> To simplify the derivation we have used the explicit values for some structure constants. This restricts the validity of Eq. (4.18) to 2 and 3 colors.

algebra and Fierz identities, the sextic vertex can be rewritten in the following simple form [47]

$$\begin{aligned} \frac{1}{3!} \langle \det_{fg} \rangle_{N_t=3} &= \frac{1}{3!} \frac{1}{N_c(N_c^2 - 1)} \int dR_{u,d,s}^3 \epsilon_{f_1 f_2 f_3} \epsilon_{g_1 g_2 g_3} \\ &\quad \left( \left( 1 - \frac{3}{2(N_c + 2)} \right) (q_{f_1}^\dagger \gamma + q_{g_1}) (q_{f_2}^\dagger \gamma + q_{g_2}) (q_{f_3}^\dagger \gamma + q_{g_3}) \right. \\ &\quad \left. + \frac{3}{8(N_c + 2)} (q_{f_1}^\dagger \gamma + q_{g_1}) (q_{f_2}^\dagger \gamma + \sigma_{\mu\nu} q_{g_2}) (q_{f_3}^\dagger \gamma + \sigma_{\mu\nu} q_{g_3}) \right) \\ &\quad + (\gamma_5 \leftrightarrow -\gamma_5). \end{aligned} \quad (4.21)$$

The first, leading in  $N_c$  term has of course the 't Hooft determinant structure. It is surprising that the subleading term has so simple form in the case of three flavors.

It can be easily demonstrated [26], for the arbitrary number of flavors, that the partition function (4.9) for large  $N_c$  is analogous to the partition function composed of 't Hooft determinants. To prove this, we evaluate the average over the color orientations and the size distribution using a cumulant expansion,

$$\begin{aligned} \left\langle \exp \left( i\chi^\dagger \int \phi^\dagger S_0^{-1} \psi + i \int \psi^\dagger S_0^{-1} \phi \chi \right) \right\rangle_{U_\rho} &= \\ \exp \left\langle -\chi^\dagger \int \phi^\dagger S_0^{-1} \psi \int \psi^\dagger S_0^{-1} \phi \chi \right\rangle_{U_\rho}, \end{aligned} \quad (4.22)$$

where the brackets  $\langle \dots \rangle_{U_\rho}$  denote averaging over the gauge group and the normalized size distribution. To leading order in  $N_c$  the higher order cumulants do not contribute. In the integrand the  $\chi^\dagger, \chi$ -variables occur as the exponent of a quadratic form, diagonal in the pseudoparticles and nondiagonal in the flavor indices. Performing this integral yields

$$\begin{aligned} \langle \det(-S^{-1}) \rangle &= \int d\psi d\psi^\dagger \exp \left( - \int \psi^\dagger S_0^{-1} \psi \right) \\ &\quad \times \prod_I \int dz_I \bar{w}(\rho_I) d\rho_I \det \left( i \left\langle \int \psi^\dagger S_0^{-1} \phi_I \int \phi_I^\dagger S_0^{-1} \psi \right\rangle_{U_\rho} \right). \end{aligned} \quad (4.23)$$

Here,  $\bar{w}(\rho)$  is the effective one-body size distribution that includes the average repulsive interaction between the pseudoparticles. The determinant in this equation is over the flavor indices and can be identified as a smeared 't Hooft determinant. For an *equal* number of instantons and anti-instantons

the partition function (4.23) *is invariant* under  $U_L(N_f) \times U_R(N_f)$  transformations of the fermion field  $\psi$ . If the number of instanton *differs* from the number of anti-instantons, the partition function *is not invariant* under  $U_A(1)$  transformations. Hence, in general it is important to account for fluctuations in the number of instantons and anti-instantons in order to account for the  $U_A(1)$  anomaly in the instanton liquid model of the QCD vacuum.

## 5. Thermal effects in the instanton vacuum

It is generally believed that QCD undergoes a phase transition at sufficiently high temperatures or densities. The nature and the character of this transition are still debated. Its existence, however, has been partly supported by lattice Monte-Carlo simulations [48,49]. This phase transition is believed to have prevailed in the early stages of the formation of the universe and is hoped to be achieved using relativistic heavy-ion colliders. It is therefore important to understand the nature and properties of QCD at high temperatures or densities.

At zero temperature, the instanton approach to the QCD ground state provides some understanding of the spontaneous breakdown of chiral symmetry [13, 15, 50], ignoring the issue of confinement. It is therefore tempting to consider the effects of the temperature on the instantonic vacuum. The existence of the instanton-like solutions for the thermal Yang-Mills theory (called caloron) allows us to extend naturally our picture of the vacuum to the  $T \neq 0$  case. Taking into account all kinds of interactions in the caloron vacuum, *i.e.*, mutual interaction between calorons, thermal gluons and fermions is a serious computational task, which, we hope, some day will be completed. Meantime, it is plausible to ask whether one could construct a kind of simple effective action, which can take into account basic long wavelength properties of the vacuum. Recently, Kanki [51] and also Diakonov and Mirlin [52] have considered the effects of temperature on the instanton vacuum. Using variational arguments, they have shown that with increasing temperatures instantons and anti-instantons are boiled off the vacuum. An extension of their analysis to include light quarks was done by Nowak, Verbaarschot and Zahed [24] and also, using the different arguments, by Ilgenfritz and Shuryak [53]. In both approaches the problem of chiral fermions in the instantonic (or rather caloric) vacuum was solved only for the case of randomly distributed pseudoparticles. Computer simulated results at zero temperature suggest that there exist strong correlation effects in the case of two and more flavors. We are aware, that these effects should be crucial for the quantitative description of the hot QCD vacuum. However, our present aim is to check if the caloric picture of the vacuum follows the general lore of the temperature dependence of the fermion



condensates, instead of studying more subtle behaviour of the thermal effects.

To study the instantons at finite temperature we adopt the same generic form for the partition function as in Chapter 2. However, in this case, due to the explicit temperature dependence, we have to make a series of modifications in the Eq. (2.6). All fields are defined on a slice of the Euclidean space, so we have to make a replacement in the all integration formulae:

$$\int_{V_4} d^4x \longrightarrow \int_0^\beta dt \int_{V_3} d^3x, \quad (5.1)$$

where  $\beta = 1/T$ . The functional integral is restricted to the fields satisfying periodic conditions

$$\begin{aligned} A_\mu(\beta, \vec{x}) &= A_\mu(0, \vec{x}) & \text{bosons} \\ \Psi(\beta, \vec{x}) &= -\Psi(0, \vec{x}) & \text{fermions} \end{aligned} \quad (5.2)$$

Therefore the integrals in momentum space should also be modified

$$\int \frac{d^4p}{(2\pi)^4} \longrightarrow \int \frac{d^3p}{(2\pi)^3} \frac{1}{\beta} \sum_n, \quad (5.3)$$

where the sum goes over Matsubara frequencies  $\omega_n$  depending on the statistics of the fields:

$$\omega_n = \begin{cases} 2n\pi/\beta & \text{bosons} \\ (2n+1)\pi/\beta & \text{fermions} \end{cases} \quad (5.4)$$

Harrington and Shepherd [54] have found the explicit instantonic-type solution with periodic boundary conditions (called caloron). Therefore all the formulae for instanton fields and instanton zero modes are still true, provided that the following replacements in the formulae (2.1) and (2.4) are made

$$\begin{aligned} \Pi &\longrightarrow \Pi_{\text{cal}} = 1 + \frac{\pi\rho^2}{\beta r} \frac{\sinh 2\pi r/\beta}{\cosh 2\pi r/\beta - \cos 2\pi t/\beta} \\ \Phi &\longrightarrow \Phi_{\text{cal}} = (\Pi_{\text{cal}} - 1) \frac{\cos \pi t/\beta}{\cosh \pi r/\beta}, \end{aligned} \quad (5.5)$$

where  $|\vec{x}| = r$ . Finally, we need to take into account the modification of the pseudoparticle density. At finite temperature, the pseudoparticle density is given by [18,55]

$$d(\rho, T) = d(\rho) \exp \left( -\frac{1}{3}\lambda^2(2N_c + N_f) + B(\lambda) \right), \quad (5.6)$$

where

$$B(\lambda) = \left(1 + \frac{1}{6}(N_c - N_f)\right)(-\ln(1 + \lambda^2/3) + 0.15(1 + 0.16\lambda^{-\frac{2}{3}})^{-8}), \quad (5.7)$$

and  $d(\rho)$  is equal to the zero temperature density (2.7). For convenience we have introduced the dimensionless variable  $\lambda \equiv \pi\rho T$ . The temperature dependence of  $B(\lambda)$  was obtained numerically by Gross, Pisarski and Yaffe [55].

Again, the fermion determinant in (2.6) can be split into a low-momentum contribution ( $\equiv \det_{\text{low}}$ ) and a high-momentum contribution ( $\equiv \det_{\text{high}}$ ). The high-momentum factor can be obtained in a standard way. The low-momentum factor is dominated by the set of zero modes

$$\det_{\text{low}}(i\gamma_\mu \widehat{\nabla}_\mu + im) = \prod_f \frac{\det(m_f^2 + D^\dagger D)}{\det(M_1^2 + D^\dagger D)}, \quad (5.8)$$

where the matrix elements of  $D$  are given by the overlaps between the *finite* temperature zero modes  $\phi_I$ . The right-handed finite temperature zero modes are given by formula (2.4) [55] but with the functions  $\Pi, \Phi$  appropriately replaced by their finite temperature counterparts (5.5).

To evaluate the low-momentum part of the fermion determinant (5.8) we use a cumulant expansion [56]. The positions and the orientations of the pseudoparticles are assumed to be distributed according to their invariant measure. Because of the formation of instanton-anti-instanton molecules [20,22], this assumption does not hold for a very dilute system. In the chirally broken phase where the pseudoparticles are in a liquid phase, we expect this assumption to provide a reasonable description of the real (unquenched) system. Even so we *do* take into account the feedback of the fermion determinant on the distribution of the sizes of the pseudoparticles. However, the fermion determinant is evaluated by a mean field approximation. We will refer to this approach as a semiquenched approximation [24]. The distribution of the sizes will be discussed later.

In the thermodynamic limit and for large  $N_c$ , we may again use the Wigner formula (3.5), but now the eigenvalues of the overlap matrix  $D$  are temperature dependent [18]

$$\bar{\nu}(\lambda(T)) = \frac{N}{\pi\kappa(T)} \left(1 - \frac{\lambda^2(T)}{4\kappa^2(T)}\right)^{\frac{1}{2}}, \quad (5.9)$$

where  $\kappa^2$  is the variance of the eigenvalues. With the help of this distribution function, the low-momentum factor of the fermion determinant reads

$$\det(m^2 + D^\dagger D) = \prod_f H(m_f), \quad (5.10a)$$

$$H(m) = \left(\frac{m}{2} + \frac{1}{2}(m^2 + 4\kappa^2)^{\frac{1}{2}}\right) \exp\left(\frac{1}{2} \frac{m - (m^2 + 4\kappa^2)^{\frac{1}{2}}}{m + (m^2 + 4\kappa^2)^{\frac{1}{2}}}\right). \quad (5.10b)$$

Under the assumption that  $1/\bar{\rho} \gg M_1 \gg \kappa$  the  $M_1$ -dependence in Eq. (2.10) cancels the  $M_1$ -dependence<sup>4</sup> of Eq. (2.11). The variance  $\kappa^2$  is proportional to the average of the trace of  $D^\dagger D$ . The averaging over the positions and the orientations can be performed analytically. The averaging over the sizes is performed by a leading-order cumulant expansion which is accurate when the distribution function is peaked. The result is

$$\kappa^2(T) = \frac{NT}{V_3 N_c} \alpha(T) \bar{\rho}^2, \quad (5.11)$$

with

$$\alpha(T) = \frac{1}{\bar{\rho}^2} \int \frac{d^3 k}{(2\pi)^3} \frac{1}{\beta} \sum_n (k^2 + \omega_n^2) (k^2 A_n^2 + \omega_n^2 B_n^2)^2, \quad (5.12)$$

and the bar denotes the averaging over the distribution of the collective coordinates. The  $\omega_n$  represent the Matsubara frequencies given by  $2\pi(n + \frac{1}{2})/\beta$ . The coefficients  $A_n$  and  $B_n$  enter in the evaluation of the density matrix of instantons and anti-instantons. They are given by

$$k A_n = \frac{1}{2\pi\bar{\rho}} \int_0^\infty 4\pi r^2 dr \int_0^\beta dt \left( \frac{\cos kr}{kr} - \frac{\sin kr}{k^2 r^2} \right) \cos \omega_n t \Pi^{\frac{1}{2}} \partial_r \frac{\phi}{\Pi}, \quad (5.13a)$$

$$\omega_n B_n = \frac{1}{2\pi\bar{\rho}} \int_0^\infty 4\pi r^2 dr \int_0^\beta dt \frac{\sin kr}{kr} \sin \omega_n t \Pi^{\frac{1}{2}} \partial_t \frac{\phi}{\Pi}. \quad (5.13b)$$

Dimensional arguments show that the function  $\alpha(T)$  depends only on the dimensionless combination  $\bar{\rho}^2 T^2$ . The shape of this function can be determined numerically. In Fig. 7 we show the result for  $\bar{\rho} = 1/3$  fm.

To evaluate the resulting partition function, we use the Feynman variational principle (see Ref. [17] for details). As a result only the average interaction  $\bar{u}_{\text{int}}$  enters in the final expressions. By a straightforward calculation [52] one obtains<sup>5</sup>

$$\bar{u}_{\text{int}} = \gamma^2 \bar{\rho}_1^2 \bar{\rho}_2^2, \quad \gamma^2 = \frac{27\pi^2}{4} \frac{N_c}{N_c^2 - 1}. \quad (5.14)$$

<sup>4</sup> Even when the double inequality is only marginally satisfied, the  $M_1$  dependence is weak. For  $T = 0$  this fact has been demonstrated in [18].

<sup>5</sup> It is assumed that the many-body forces do not play an important role at the instanton densities relevant for the description of the QCD vacuum. Again, this assumption will be justified *a posteriori* by the result that the instanton medium is dilute.

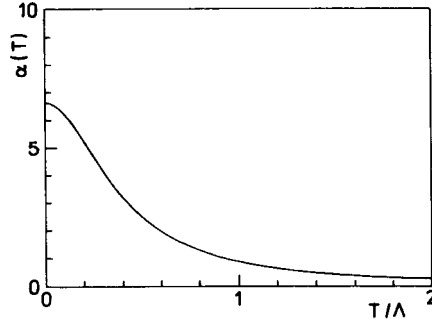


Fig. 7. Temperature dependence of the eigenvalues of the overlap matrix  $D$  as given by the function  $\alpha(T)$  defined in Eq. (5.12). The curve was evaluated for  $\bar{\rho} = 1/3$  fm.

Note that the average interaction does not depend on the chirality of the instantons, and that the coefficient  $\gamma^2$  is temperature independent. Using  $\mu(\rho, T)$  as a variational one-body density to account for the two-body interaction, the partition function is bounded from below by

$$\sum_{N_+, N_-} \frac{1}{N_+! N_-!} \int \prod_I d\Omega_I \mu(\rho_I, T) \exp \left( -\beta(\bar{\rho}) \sum_{I < J} \bar{u}_{\text{int}}(I, J) - \sum_I \ln \mu(\rho_I, T) / d(\rho_I, T) \right), \quad (5.15)$$

The function  $\mu$  is determined variationally. We find that the instantons and the anti-instantons are distributed according to the same distribution function  $\mu$ ,

$$\mu(\rho, T) = d(\rho, T) \exp \left( \overline{\ln \mu / d} + \frac{1}{2} \sum_f \frac{1}{H} \frac{\partial H}{\partial \bar{\rho}} (\rho - \bar{\rho}) - \frac{\beta(\bar{\rho}) \gamma^2 T N}{V_3} \bar{\rho}^2 (\rho^2 - \bar{\rho}^2) \right). \quad (5.16)$$

The term involving  $H$  is due to the  $\mu$ -dependence of the average size. The argument of the running coupling constant is fixed after minimization with respect to  $\mu$ , and is given by  $\bar{\rho}^2 \Lambda^2$ . The average squared size is determined selfconsistently from

$$\bar{\rho}^2 = \frac{\int d\rho \mu(\rho) \rho^2}{\int d\rho \mu(\rho)}, \quad (5.17)$$

and  $\bar{\rho}$  is defined by  $(\bar{\rho}^2)^{\frac{1}{2}}$ .

The free energy  $F \equiv \ln Z$  is given by [24]

$$F(T) = N \left( -\ln \frac{n(T)}{2\Lambda^4} - \frac{1}{2} \sum_f \frac{1}{H} \frac{\partial H}{\partial \bar{\rho}} \bar{\rho} + \frac{1}{2} \beta(\bar{\rho}) \gamma^2 n(T) \bar{\rho}^2 \right) + \ln \int d\rho d(\rho, T) \Lambda^4 \exp \left( \frac{1}{2} \sum_f \frac{1}{H} \frac{\partial H}{\partial \bar{\rho}} \rho - \beta(\bar{\rho}) \gamma^2 n(T) \bar{\rho}^2 \right), \quad (5.18)$$

where the density of pseudoparticles  $NT/V_3$  is denoted by  $n(T)$ . In the thermodynamic limit  $n(T)$  is determined by the value of  $N$  where  $F$  has its maximum. In the dilute limit the extremum can be determined analytically. In this limit the density dependence of the free energy density  $\mathcal{F}$  is given by

$$\mathcal{F} = n(T)(c(T) + (\frac{N_f}{2} - 1) \ln \frac{n(T)}{\Lambda^4}), \quad \frac{n(T)}{\Lambda^4} \ll 1, \quad (5.19)$$

where  $c(T)$  is a temperature dependent constant. The free energy density at the extremum is  $(N_f/2 - 1)n(T)/\Lambda^4$ . In the three-flavor case, the free energy becomes negative in the dilute limit leading to a first order phase transition to the trivial solution  $n(T) = 0$ . In the two-flavor case, the free energy is zero in the dilute limit which results in a second order phase transition. In the one-flavor case, the free energy for the nontrivial solution is always positive and no phase transition takes place. This behavior is illustrated in Fig. 8 where we show the ratio  $F(T)/F(0)$  as a function of the temperature  $T$  for one, two and three massless flavors.

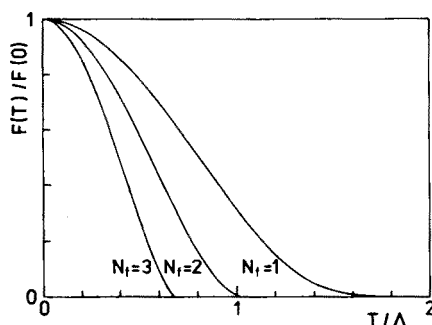


Fig. 8. Ratio of the free energy  $F(T)$  to  $F(0)$  as a function of the dimensionless temperature  $T/\Lambda$ . Here the quarks are massless.

The derivative  $\partial_T F(T)$  is discontinuous at the critical point for three flavors only. The free energy per particle  $F(0)/N$  is 2.17, 1.21 and 0.672 for  $N_f = 1$ , 2 and 3, respectively.

To reproduce the phenomenological value of the gluon condensate, we have chosen the coupling constant in the pre-exponential factor to be  $8\pi^2/g^2 = -b \ln 0.1$ . The value of  $\Lambda_{PV}$  is fixed by requiring that the gluon condensate at zero temperature ( $\langle F_{\mu\nu}^2 \rangle = (190 \text{ MeV})^4$ ) is saturated by  $NT/V_3$ . In the three flavor-case, the latter quantity is equal to  $0.2257\Lambda^4$  which yields a value of  $\Lambda_{PV} = 275 \text{ MeV}$ . The average size of the pseudoparticles at  $T = 0$  is equal to  $0.36 \text{ fm}$ , whereas the distance between the pseudoparticles defined by  $(NT/V_3)^{-1/4}$ , is equal to  $1.45 \text{ fm}$ . This demonstrates that our system is dilute. The validity of the semiclassical limit is guaranteed by the value of the running coupling constant,  $8\pi/g^2 = -b \ln \bar{\rho}\Lambda = 6.4$ . Similar numerical values have been obtained for one and two flavors.

Mean-field approach presented in Chapter 4, easily generalizes to non-zero temperatures by replacing the zero temperature zero modes by zero modes corresponding to the caloron solution, and replacing the integral over the four-momentum by its finite temperature counterpart. As gap equation we obtain (*cf.* (4.15) )

$$\int \frac{d^3k}{(2\pi)^3} \frac{1}{\beta} \sum_n \frac{M^2(\vec{k}, \omega_n)}{k^2 + \omega_n^2 + M^2(\vec{k}, \omega_n)} = \frac{NT}{4V_3N_c}, \quad (5.20)$$

where the momentum-dependent effective mass is defined by (*cf.* (4.16))

$$M(\vec{k}, \omega_n) = \frac{\epsilon NT}{2V_3N_c} (k^2 + \omega_n^2)(k^2 A_n^2 + \omega_n^2 B_n^2). \quad (5.21)$$

Also the result for the chiral condensate is a straightforward generalization of the zero temperature case

$$\langle \bar{q}q \rangle = -4N_c \int \frac{d^3k}{(2\pi)^3} \frac{1}{\beta} \sum_n \frac{M(\vec{k}, \omega_n)}{\vec{k}^2 + \omega_n^2 + M^2(\vec{k}, \omega_n)}. \quad (5.22)$$

One can show that the chiral condensate and the constituent quark mass depend only on the dimensionless combinations  $n(T)\rho^4$  and  $\bar{\rho}^2 T^2$ .

The value of  $\epsilon$  is determined by solving Eq. (5.20) iteratively. This solution enables us to calculate the constituent mass  $M(\vec{k} = 0, \omega_{n=0})$  and the chiral condensate  $\langle \bar{q}q \rangle$ . Their temperature dependence for one, two and three flavors is displayed in Fig. 9 and Fig. 10.

We clearly see that the order of the phase transition depends on the number of flavors. For low temperatures the chiral condensate is almost independent of the temperature. This is the result of two opposing effects. The chiral condensate obtained from Eqs (5.20), (5.21) and (5.22) increases both with temperature and with density. However, the actual density as

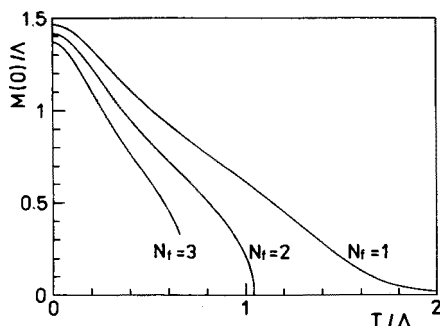


Fig. 9. Constituent mass  $M(0) \equiv M(\vec{k} = 0, \omega_n=0)$  in units of  $\Lambda$  as a function of  $T/\Lambda$ .

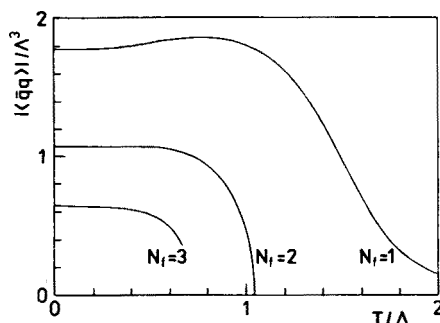


Fig. 10. Chiral condensate  $\langle \bar{q}q \rangle \Lambda^3$  as a function of the temperature in units of  $\Lambda$ .

obtained from the free energy (Eq. (5.18)) decreases with increasing temperature. With the numerical parameters quoted above the  $N_f = 3$  values at zero temperature of the constituent quark mass and the chiral condensate are equal to 370 MeV and  $(237 \text{ MeV})^3$ , respectively. The critical temperature in this case is 180 MeV. These values are in rough agreement with values obtained from a phenomenological analysis.

In conclusion, the order of the chiral phase transition in an instanton model for the QCD vacuum depends sensitively on the number of massless flavors. We find a second order phase transition in the two-flavor case and a first order phase transition for the three-flavor case. We would like to stress once more, that these results were obtained in semiquenched approach, where large part of the important fermion correlations were neglected.

## 6. Effective lagrangians

At low-energy and in the large  $N_c$  limit flavor dynamics is generic (see for example Refs [57,58]). To leading order, the light pseudoscalar mesons

decouple from the heavier (scalar and pseudoscalar) glueballs. The dynamics can be described in the context of nonlinear-sigma models suitably coupled to heavy scalar and pseudoscalar glueball fields. The generic form of flavor dynamics in the long-wavelength approximation is reminiscent to the Landau–Ginzburg construction.

To leading order in  $N_c$ , the resulting partition function is equivalent to the partition function of constituent quarks interacting via 't Hooft vertices [13]. After a suitable coarse graining, we show that our effective action (4.10) is consistent with the ones discussed in the literature and based on nonlinear sigma-models. In our effective action the role of the glueballs is played by the instanton and anti-instanton densities. We show that the effective action satisfies both the chiral anomaly and the scale anomaly [26]. The latter is directly related to the compressibility of the instanton liquid.

To show that the effective action implied by the partition function given in Eq. (4.10) is reminiscent to an effective action proposed some time ago by Schechter *et al.* [58] we will apply the coarse-graining technique. For this we choose to rewrite the integral over the positions of the instantons as an integral over the density of the instantons by allowing for the number of instanton and anti-instanton to *change*. To achieve this we partition the total Euclidean volume  $V$  in blocks  $\Delta V_i$  containing  $n^+(z_i)$  instantons and  $n^-(z_i)$  anti-instantons, where  $z_i$  denotes the position of the block  $\Delta V_i$ . Assuming a sufficient amount of coarse graining we have

$$\int \prod_I dz_I \bar{w}(\rho_I) d\rho_I F(z_I) = \int \prod_{\Delta V_i} dn^+(z_i) dn^-(z_i) F_+^{n^+(z_i)}(z_i) F_-^{n^-(z_i)}(z_i). \quad (6.1)$$

In the limit  $\Delta V \rightarrow 0$  this integral becomes a functional integral,

$$\int \prod_z dn^+(z) dn^-(z) F_+^{n^+(z)}(z) F_-^{n^-(z)}(z). \quad (6.2)$$

So far we have only discussed the leading term in the grand-partition function: the instanton density is fixed. In what follows, we will also include fluctuations about this density. (In general, in the grand-partition function these fluctuations are induced through correlations in the collective variables.) The attitude we are taking here is that the mean-field approximation for the liquid phase provides a good description for the bulk parameters of the QCD vacuum. Therefore we expect that correlations in the density of instantons can be described by few low order moments.



With this in mind, we take the pseudoparticle densities at different space-time points to be uncorrelated. For the pseudoparticles densities at the same space-time points we have

$$\begin{aligned}\langle\langle n^+(z) \rangle\rangle &= \langle\langle n^-(z) \rangle\rangle = \frac{1}{2} \frac{N}{V}, \\ \langle\langle n^+(z) n^-(z) \rangle\rangle &= \langle\langle n^+(z) \rangle\rangle \langle\langle n^-(z) \rangle\rangle.\end{aligned}\quad (6.3)$$

The functional average over the distribution of the pseudoparticles has been denoted by  $\langle\langle \dots \rangle\rangle$ . Since different pseudoparticles are uncorrelated we have

$$\int d^4z \langle\langle (n^+(z) - n^-(z))^2 \rangle\rangle = \frac{N}{V}. \quad (6.4)$$

Thus the variance in the number difference is of order  $N_c$ . The variance of the total number of instantons and anti-instantons in the vacuum

$$\sigma^2 = \int d^4z \left\langle \left\langle \left( n^+(z) + n^-(z) - \frac{N}{V} \right)^2 \right\rangle \right\rangle \quad (6.5)$$

is related to the compressibility of the instanton liquid. Both the variational calculations and low energy theorems indicate that  $\sigma^2 \sim N_c^0$ . In our case it will be fixed by the requirement that the scale anomaly is correctly reproduced at tree level. This requirement is consistent with the low energy theorems. Therefore, we expect  $\sigma^2/(N/V) \sim N_c^{-1}$  to vanish in the large  $N_c$  limit, indicating a sharply peaked distribution in the total instanton number density.

Using the coarse grained version of (4.10) and (6.3 and 6.5), we obtain the following effective action for the instanton liquid state

$$\begin{aligned}W &= \frac{1}{\sigma^2} \frac{N}{V} \int d^4z \left( n^+(z) + n^-(z) \right) \left( \ln \frac{n^+(z) + n^-(z)}{N/V} - 1 \right) \\ &+ \frac{V}{2N} \int d^4z \left( n^+(z) - n^-(z) \right)^2 \\ &+ \int d^4z \left( \psi^\dagger S_0^{-1} \psi - n^+(z) \ln \det_+(z) - n^-(z) \ln \det_-(z) \right),\end{aligned}\quad (6.6)$$

where we have used the shorthand notation for the smeared 't Hooft determinants<sup>6</sup> (the  $z$  dependence relates to the global position of an instanton or anti-instanton).

$$\det_\pm(z) = \frac{1}{N_f!} \det_{fg} \left( m - \frac{1}{2i} \left\langle \int \psi^\dagger f S_0^{-1} \phi_\pm \int \phi_\pm^\dagger S_0^{-1} \psi g \right\rangle_{U_\rho} \right). \quad (6.7)$$

<sup>6</sup> The formula presented below is a generalization of the formula (4.9) to the case of massive quarks. For more details we refer to [26].

The fluctuations in the number densities in (6.6) stand for the “gluonic” contribution to the effective action. The distribution of the difference  $n^+(z) - n^-(z)$  is Gaussian with a width given by (6.4). The distribution of the sum  $n^+(z) + n^-(z)$  is logarithmic and consistent with ((6.3) and (6.4)) in the Gaussian approximation (to be justified below)<sup>7</sup>. The latter is exact in the large  $N_c$  limit.

Under an infinitesimal  $U_A(1)$  transformation  $\psi(z) \rightarrow (1 + i\alpha(z)\gamma_5)\psi(z)$  where  $\alpha$  varies slowly on the scale of the size of the instantons, we have

$$\partial_\mu j_{5\mu} = -2N_f(n^+(z) - n^-(z)). \quad (6.8)$$

The axial singlet current vanishes in a  $CP$  symmetric vacuum. Since the variance of the number difference (6.4) (topological susceptibility) does not vanish, we expect (6.8) to generate nonvanishing matrix elements between the vacuum (topologically neutral state) and pseudoscalar singlet excitations (*e.g.*  $\eta_0$ ). This result is consistent with QCD.

To exhibit the scale anomaly, let  $\rho \rightarrow \lambda^{-1}\rho$ ,  $\psi(z) \rightarrow \lambda^{\frac{1}{2}}\psi(\lambda z)$ , and  $n^\pm(z) \rightarrow \lambda^4 n^\pm(\lambda z)$  in (23). Under this transformation the first term in the effective action (6.6) transforms as

$$\begin{aligned} \frac{\delta}{\delta\lambda} \left( \frac{1}{\sigma^2} \int d^4z (n^+(z) + n^-(z)) \left( \ln \frac{n^+(z) + n^-(z)}{\frac{N}{V}} - 1 \right) \right) \\ = + \frac{4}{\sigma^2} (n^+(z) + n^-(z)). \end{aligned} \quad (6.9)$$

It follows that the divergence of the dilatation current does not vanish at tree level (*i.e.*, only classical instanton and anti-instanton configurations). The result is

$$\partial_\mu j_\mu^{\text{dil}} = \left( \frac{4}{\sigma^2} \left( \frac{N}{V} \right) + \mathcal{O}(1/\ln^2(\rho\Lambda)) \right) (n^+(z) + n^-(z)). \quad (6.10)$$

The first term is the gluonic contribution to the trace anomaly, while the second term is the fermionic contribution. The latter contribution is obtained by using the one-loop beta function in the size distribution  $\bar{w}(\rho)$ . Since it is subleading in  $1/N_c$ , we will not take it into account any further.

If we were to identify the instanton density  $N/V$  in the liquid phase with the value of the gluon condensate  $\langle 0|F_{\mu\nu}^2/32\pi^2|0\rangle$ , then a comparison of the vacuum expectation value of (6.10) with the usual QCD trace anomaly yields the following equation for the variance in the large  $N_c$  limit

$$\sigma^2 = \frac{4}{b} \frac{N}{V} \quad (6.11)$$

<sup>7</sup> The logarithmic choice is also motivated by the Stirling form of the pre-exponential factorials in the grand-partition function.

where  $b = 11N_c/3$ . This result was first obtained in [17] in the instanton liquid using a detailed variational calculation. Notice that in the large  $N_c$  limit the instanton liquid becomes incompressible. For  $N_c = 3$ , the ratio  $\sigma^2/(N/V) = 4/11$  indicates a peaked distribution in the total number of instantons. *A posteriori*, this result justifies the use of a Gaussian approximation for the distribution of the total density of the pseudoparticles.

By introducing the coarse grained fields  $H(z) = \frac{1}{2}(n^+(z) + n^-(z))$  (scalar glueball) and  $Q(z) = \frac{1}{2}(n^+(z) - n^-(z))$  (pseudoscalar glueball), the grand-canonical partition function  $\Xi$  corresponding to the effective action (6.6) can be rewritten as

$$\Xi = \int d\psi d\psi^\dagger \exp \left( - \int \psi^\dagger S_0^{-1} \psi \right) \int \prod_z 2dH(z)dQ(z)W(H, Q) \times (\det_+(z) \det_-(z))^{H(z)} \left( \frac{\det_+(z)}{\det_-(z)} \right)^{Q(z)}. \quad (6.12)$$

The instanton and anti-instanton distribution functional  $W(H, Q)$  can be read immediately from the effective action (6.6). It is logarithmic in  $H$  and Gaussian in  $Q$ . Notice that the combination  $(\det_+ \det_-)$  is  $U_A(1)$  invariant, while the combination  $(\det_+ / \det_-)$  breaks  $U_A(1)$ . As mentioned above, the fluctuations in the number difference  $Q$  are at the origin of the  $U_A(1)$  anomaly. In general the distribution functional  $W(H, Q)$  is more complicated than indicated above. However, for a system of instantons and anti-instantons in the liquid phase, we expect the above approximations to be satisfactory. These approximations should be contrasted with the dilute gas approximation where the collective variables decouple. In this case  $n^+$  and  $n^-$  are uncorrelated, and we find that the compressibility for the total number of pseudoparticles is equal to one. However, this case does not have a well behaved infrared limit. Therefore it is clear that the 't Hooft effective actions that have been derived with the dilute gas approximation can be at best qualitative.

To describe the long wavelength pseudoscalar excitations, we can either study source-source correlators in the vacuum described by (6.7), or equivalently bosonize the fermionic degrees of freedom in (6.7) [27]. To achieve this we use the completeness relation

$$1 = \int d\pi^\pm \int dP^\pm \exp -i \int P^\pm (\pi^\pm - \langle \psi^\dagger S_0^{-1} \phi_\pm \phi_\pm^\dagger S_0^{-1} \psi \rangle), \quad (6.13)$$

where  $P^\pm$  are the auxiliary fields associated to the pseudoscalar fields  $\pi^\pm$ . The fields  $\pi^\pm$  are eliminated with the help of the mean field equations for fixed values of  $P^\pm$ . In this way the gaussian fluctuations in  $\pi^\pm$  are included in the partition function.

After bosonization the fermionic part of the effective action takes the following form

$$W_F = -N_c \sum_f \text{Tr} \ln \left( \hat{k} + im + iP^+(k-l) \left( 1 + \frac{im\hat{k}}{k^2} \right) \gamma_5^+ \left( 1 + \frac{im\hat{l}}{l^2} \right) \sqrt{M_k M_l} \right. \\ \left. + iP^-(k-l) \left( 1 + \frac{im\hat{k}}{k^2} \right) \gamma_5^- \left( 1 + \frac{im\hat{l}}{l^2} \right) \sqrt{M_k M_l} \right). \quad (6.14)$$

The trace is over the Dirac indices and the four momenta. In order to distinguish the Goldstone modes from the massive modes we consider Eq. (6.13) for zero quark masses. Then the action is invariant under the global transformation

$$P^+ \rightarrow \exp \left( + \frac{i\kappa}{2} \right) P^+ \exp \left( + \frac{i\kappa}{2} \right), \\ P^- \rightarrow \exp \left( - \frac{i\kappa}{2} \right) P^- \exp \left( - \frac{i\kappa}{2} \right). \quad (6.15)$$

This suggests the parametrization

$$P^\pm = \exp \left( \pm \frac{i\kappa}{2} \right) \sigma \exp \left( \pm \frac{i\kappa}{2} \right), \quad (6.16)$$

where  $\kappa$  and  $\sigma$  are  $N_f \times N_f$  Hermitean matrices. The  $\kappa$ -variables can be identified as the pseudoscalar Goldstone modes. The  $\sigma$ -variables are massive and can be eliminated with the help of the saddle point equations. The lowest order the saddle point solution  $\bar{\sigma}$  does not depend on the quark masses. We can set  $\bar{\sigma} = 1$  after a suitable redefinition of the constituent mass  $M_k$  in (6.14). We need only to expand the logarithm up to first order to obtain all terms of  $\mathcal{O}(\kappa^2)$  at zero momentum and to leading order in the current quark masses. To this order the contributing terms depend only on the following combination of  $m$  and  $\kappa$ ,

$$\text{Tr} \left( m(1 - \frac{1}{2}\kappa^2) \right). \quad (6.17)$$

This expression can be rewritten as

$$2m + m_s \\ - \frac{1}{2} \left( \frac{4m}{3} \left( \kappa_0 + \frac{1}{\sqrt{2}} \kappa_8 \right)^2 + \frac{2m_s}{3} \left( \kappa_0 - \sqrt{2} \kappa_8 \right)^2 \right. \\ \left. + 2m \sum_{k=1,2,3} \kappa_k^2 + (m + m_s) \sum_{k=4,5,6,7} \kappa_k^2 \right), \quad (6.18)$$

where we have used the decomposition  $\kappa = \sum_{k=0}^8 \kappa_k \lambda_k$ . For zero momentum pseudoscalar excitations (constant  $\kappa_f$ ) we can immediately write down the relations

$$\begin{aligned} \frac{\partial^2 W_F}{\partial \kappa_k^2} &= -m \frac{\partial W_F}{\partial m} + \mathcal{O}(m^2), \quad k = 1, 2, 3 \\ \frac{\partial^2 W_F}{\partial \kappa_k^2} &= -\frac{1}{2}(m + m_s) \frac{\partial W_F}{\partial m} + \mathcal{O}(m^2), \quad k = 4, 5, 6, 7, \end{aligned} \quad (6.19)$$

and similar relations involving the  $\kappa_0$  and  $\kappa_8$  fields. The derivatives with respect<sup>8</sup> to  $m$  are related to the Euclidean condensate by

$$\frac{\partial W_F}{\partial m} = -i \langle \psi^\dagger \psi \rangle \quad (6.20)$$

from which we immediately obtain the PCAC relation. Note that to the order in  $m$  we are working, the chiral condensate does not depend of the flavor.

To investigate the momentum content of the pseudoscalars consider first the  $\kappa_0$  and  $\kappa_8$  excitations, which can be identified as the  $\eta'$  and the  $\eta$  field, respectively. Inserting (6.16) in (6.14) and expanding around zero momentum gives (momentum integration understood)

$$\begin{aligned} &\frac{1}{2} f^2 p^2 (\eta^2 + \eta'^2) \\ &+ i \frac{\langle \psi^\dagger \psi \rangle_E}{2} \left( \eta'^2 \left( \frac{2}{3} m + \frac{1}{3} m_s \right) + \eta^2 \left( \frac{1}{3} m + \frac{2}{3} m_s \right) + \eta \eta' \frac{2\sqrt{2}}{3} (m - m_s) \right). \end{aligned} \quad (6.21)$$

where the quark condensate and the pseudoscalar decay constant  $f$

$$\begin{aligned} f^2 &= \lim_{q^2 \rightarrow 0} \frac{1}{q^2} 4N_c \int \frac{d^4 k}{(2\pi)^4} \frac{(M(k_+)k_- - M(k_-)k_+)^2}{(k_+^2 + M^2(k_+))(k_-^2 + M^2(k_-))} \\ k_\pm &= k \pm q/2 \end{aligned} \quad (6.22)$$

are evaluated in the chiral limit. For the  $\pi$  and the  $K$  excitations in (6.16), we find the mass relations

$$m_\pi^2 = -2m \langle \bar{\psi} \psi \rangle / f^2 \quad (6.23)$$

$$m_K^2 = -(m + m_s) \langle \bar{\psi} \psi \rangle / f^2. \quad (6.24)$$

<sup>8</sup> When we differentiate with respect to  $m$ , we take into account that  $m$  is the average of  $m_u$  and  $m_d$ . By the derivative with respect to  $m$  we mean the derivative either with respect to  $m_u$  or with respect to  $m_d$ .

We have explicitly used the fact that  $\langle \bar{\psi}\psi \rangle = -i\langle \psi^+ \psi \rangle_E$  between the Euclidean and Minkowski condensates. To account for the mass of the  $\eta'$  we have to add the gluonic part due to the fluctuations in the topological susceptibility. We have shown that the terms proportional to the difference  $n^+(z) - n^-(z)$  in the pseudoparticle densities are given by

$$W_G = \frac{V}{2N} \int d^4z \left( n^+(z) - n^-(z) \right)^2 - i\sqrt{2N_f} \int d^4z \left( n^+(z) - n^-(z) \right) \eta'. \quad (6.25)$$

This gives rise to a gluonic contribution to be added to the fermionic contribution (6.14). Integrating out the pseudoparticle difference, we obtain the following result for the second order expansion in the  $\eta - \eta'$ -fields of our effective action (momentum integration understood)

$$\begin{aligned} & \frac{1}{2} f^2 p^2 \left( \eta^2 + \eta'^2 \right) + N_f \frac{N}{V} \eta'^2 \\ & + \frac{1}{2} f^2 \eta^2 \left( \frac{4}{3} m_K^2 - \frac{1}{3} m_\pi^2 \right) + \frac{1}{2} f^2 \eta'^2 \left( \frac{2}{3} m_K^2 + \frac{1}{3} m_\pi^2 \right) + \frac{1}{2} f^2 \eta \eta' \frac{4\sqrt{2}}{3} (m_\pi^2 - m_K^2). \end{aligned} \quad (6.26)$$

This result coincides with the result obtained by Veneziano [59]. In particular, for zero quark masses, we obtain the Witten-Veneziano [59,60] formula.

Using the standard instanton liquid model parameters  $N/V = 1 \text{ fm}^{-4}$  and  $\bar{\rho} = \frac{1}{3} \text{ fm}$  we obtain for the constituent mass  $M(0) = 345 \text{ MeV}$ , for the condensate  $\langle \bar{\psi}\psi \rangle = (255 \text{ MeV})^3$  and for the decay constant  $f = 91 \text{ MeV}$ . The current masses  $m = 5 \text{ MeV}$  and  $m_s = 120 \text{ MeV}$  reproduce the experimental values of  $m_\pi$  and  $m_K$ . Diagonalization of the mass matrix given in (6.26) yields [27]  $m_\eta = 527 \text{ MeV}$  (exp.:  $549 \text{ MeV}$ ) and  $m_{\eta'} = 1172 \text{ MeV}$  (exp.:  $958 \text{ MeV}$ ). The corresponding mixing angle comes out to be  $\theta = -11.5^\circ$  (exp.:  $\approx -20^\circ$  [61]).

## 7. Summary and conclusions

Our aim was to present in a self-consistent way the variety of the approaches to the physics of light quarks propagating through the vacuum populated by the instantonic fluctuations. The most important effect of these propagation is a phenomenon of the chiral symmetry breakdown. This effect is a consequence of the delocalization of the zero modes in the infinite and disordered configuration of instantons resembling a liquid phase. The nature of this mechanism is generic. One may draw many analogies to the stochastic configurations in solid states physics [37], like percolation problems or Mott insulator-conductor phase transition. It can be proven, that

the delocalization mechanism is generated mostly by stochastic properties of the ensemble of field configurations supporting the zero modes [18,22,62]. Self-dual fields are preferred candidates due to their stability with respect to quantum fluctuations and due to the presence of the zero modes [62]. The basics of the instanton vacuum formalism was presented in Chapter 2. In Chapter 3 we demonstrated the way computer simulation on the ensemble of the instantons interacting with light quarks could be performed. Generally, the simulations described in this chapter support the qualitative scenario described above. There are, however, some unexpected results coming from the recent, largest-to-date instanton vacuum simulation [23]. First, it seems that there is a crucial difference between the vacuum structure for two and three massless flavors. At physical densities,  $N_f = 2$  simulation demonstrates the liquid phase, whereas, at the same density, for three flavors chiral symmetry remains unbroken. The origin of this behaviour is unknown and requires further studies. One may wonder whether the interaction via the multifermion vertices does not require the inclusion of some kind of quark-quark correlations for large number of flavors. Of course, such an effect may be a genuine feature of the vacuum. It does not contradict the experimental data, since in reality the mass of the strange quark is not, by any means, a small number. The direct simulation with massive strange quark and two light other flavors gives the chiral symmetry breakdown at physical density and provides the data comparable to experiment [23]. At very high densities,  $N_f = 3$  system seems to prefer the crystalline form. Studies of the instanton model at large densities require some extra care. First, the dilute gas approximation for the quantum corrections is no longer valid in this region. Second, the concentration of large topological charge in a relatively small volume may require the inclusion in the ansatz field configurations with topological charges greater than one. Third, the boundary condition effect and the ansatz dependence are not yet fully investigated in this case.

It is tempting to compare the results of the simulation to the Monte-Carlo results obtained in lattice QCD simulation. Despite the formal similarity of the technical tools used in both kinds of simulation, the approach is quite different and therefore the comparison is not straightforward. Instanton vacuum picture assumes *a priori*, that there exists a subclass of the gluonic configurations (*i.e.*, instantons), which is most important from the point of view of the chiral symmetry breaking. In lattice calculations, all gluonic fluctuations are treated at the same footing. Because of the random character of the gauge configurations generated in course of simulation, it is difficult to identify which particular gauge configuration is dominating the partition function. Another difficulty is related to the study of the chiral symmetry breaking on the lattice, which require so called “staggered fermion” formalism. An introduction of  $N_f$  kinds of fermions on the lattice

leads to  $4N_f$  kinds of fermions in the continuum limit. Finally, the notion of topological quantities defined on the array of isolated points requires careful analysis and even then becomes biased by ambiguities. An additional difficulty is related to the fact, that topological fluctuations are large ( $1/3$  fm), whereas the present lattices are rather small ( $1$  fm<sup>4</sup>). Despite all the problems, progress on the direct study of the topological properties on the lattice is growing. We would like to refer here to the recent analysis of a lattice simulation [63], in which the authors provide convincing evidence for the topological origin of the chiral symmetry breaking. Their calculation of the topological susceptibility on the lattice is in striking agreement with the value extracted from Witten Veneziano formula, which may be understood in the long wavelength limit of the instanton liquid model. The molecular instanton-antiinstanton configuration was also observed in the chirally symmetric phase in lattice Monte Carlo simulation done in [64]. The dependence of the distance between the pseudoparticle as a function of the mass of a light quark agrees with the dependence observed for molecules in the instantonic vacuum picture [22]. We hope, that another challenging comparison will be soon available due to enormous progress in lattice gauge calculations. Especially interesting are APE project and Teraflop project [65]. If successfully completed, one may expect as soon as in 1993 the quenched QCD simulations on the lattices as big as  $128^3 \times 256$  and full QCD simulations on a lattice  $32^3 \times 64$ . The amount of instantons "packed" in such big lattices is at least comparable to the instantonic simulations.

The comparison between the thermal instantonic vacuum and the finite  $T$  lattice simulations is much more awkward. Present lattice simulations suggest that the deconfinement and chiral symmetry restoration happens at the same temperature [66]. Instanton vacuum picture, on the other side, ignores the fluctuations leading to confinement. The tacit assumption in this picture is that both mechanisms may be unrelated and that QCD may undergo two separate transitions at different temperatures. The deconfining configurations are suspected to be larger scale fluctuations, but their nature and possible interrelations to instantons are unknown. The order of the thermal phase transition is not firmly established. At present, most finite temperature lattice calculations with light fermions are performed on rather small lattices and the finite size effects are not fully understood. In case of  $N_f > 4$  the transition is of the first order. A common folklore is that for  $2 \leq N_f \leq 4$  the transition is of the first order. Universality arguments by Pisarski and Wilczek [67] indicate that there is no chiral transition for one flavor, the transition is of the first order for flavor number greater or equal to three, and in the case  $N_f = 2$  the transition *may be* of the second order. This scenario for the flavor dependence seems to be confirmed by our mean-field calculations for the finite-temperature instantons [24]. However,



these calculations ignore the fermionic correlations which are so crucial in the  $T = 0$  case, therefore the mean-field results should be treated with some reserve. Large scale simulation for thermal instantons is now under progress [35]. Large statistics studies of the finite temperature QCD for lattices  $32^3 \times N_T$  for  $N_T$  as large as 16 were being proposed as well [65]. We hope this parallel progress will help in understanding this important issue.

As an alternative to the simulation we presented here the mean-field approach to the instantonic vacuum. The basic assumption in this picture is that instantons are distributed homogeneously in space and are located on color manifold according to the invariant measure [17]. This picture obviously breaks down for the molecular phase, where instantons are pair-wise correlated in space and color, but seems to be valid in a liquid, chirally broken phase. Exact analytical results are available only in one flavor case or in the limit  $N_c \rightarrow \infty$ , but in other cases one may obtain the approximate solutions using saddle point approximation. In Chapter 4 we have presented the mean-field formalism for the partition function of the ensemble of instantons interacting with massless quarks. The functional formalism adopted there allowed us to present the original construction by Diakonov and Petrov [18] in a simple and suggestive form [26,22]. The formalism can be also generalized in a straightforward way to the finite temperature case [24]. Basically, it requires rewriting of "many body physics" taking place in the instanton medium using the plane wave basis for the quark fields. In this form, one can extract immediately an effective action for the delocalized fermions once the statistical averaging is performed. Averaging over the collective positions yields momentum conservation, whereas averaging over color orientations singles out color singlets and restores the local gauge invariance. The dynamics is described by a Nambu–Jona-Lasinio [68] type model with smeared 't Hooft's interactions [26]. The purpose of Chapter 6 was to demonstrate, that in the long wavelength limit our effective action is generic with effective actions obtained from large  $N_c$  arguments. Bulk correlations in the liquid state were included by using the coarse-graining technique. Local variations in the density of instantons were identified with the scalar glueball field, whereas local variations in the topological susceptibility were generating the pseudoscalar glueball. Construction of the action guaranties that chiral and scale anomalies are reproduced. Finally, we have discussed some phenomenological consequences of the adopted action. We demonstrated that in the chiral limit the  $\pi$ ,  $K$  and  $\eta$  particles are Goldstone modes in the instanton liquid state, as first noted in [18], whereas the  $\eta'$  particles are heavy due to the explicit breaking of the  $U_A(1)$  anomaly by instantons. The calculated parameters for the pseudoscalar nonet observables are in good agreement with the data [27].

To sum up, let us mention some prospects and possible improvements in the instanton liquid picture. Full simulation of the grand canonical ensemble is still lacking. The studies of the thermal properties of the medium are still at the qualitative level only. The implementation of the non-zero modes in one instanton-background quark propagator may be possible (this was done recently in the mean field approximation [69]). It is challenging to find the better ansatz for the instanton configuration. The study of the quantum corrections around the ansätze does not go beyond the dilute medium approximation. Last but not least, larger-scale simulations with higher statistics are needed. Let us note at this point, that the up-to date results in the instanton vacuum picture did not only reproduce successfully most of the bulk properties of the vacuum, but also provided encouraging results in the studies of the vector, axial [70] and heavy flavor mesons [71]. Even such subtle effects as flavor mixings [22,25], OZI rule violation [72] and proton spin problem [73] were analyzed with the help of the instanton vacuum picture. All told, we believe that further investigation in this field is of great interest.

We hope that the review of the instanton liquid model presented in this paper provides the reader with some insight on the character of the vacuum and mechanism of the chiral symmetry breaking, offers him the qualitative and as well as quantitative framework for studies of the low energy physics and may convince him that instanton vacuum picture can successfully supplement the lattice gauge calculations.

This paper is a broad resumé of a series of papers written at Stony Brook in a fruitful collaboration with Jac Verbaarschot and Ismail Zahed, which has shaped most of my understanding of the subject. During the course of this work I benefited also from discussions with Reinhard Alkofer (who also collaborated with us on pseudoscalar nonet), Mitia Diakonov, Stefano Forte, Hans Hansson, Michał Praszalowicz, George Ripka, Edward Shuryak, Alosha Yung and Wolfram Weise. I would like to thank Prof. Andrzej Bialas for useful suggestions and a critical reading of the manuscript. My special gratitude is devoted to Mannque Rho for his constant help and encouragement throughout this work, and to Gerry Brown for prompting me to the physics of instantons.

## Appendix A

### *A.1. Euclidean space conventions*

We present here formulae which allow the transition from Minkowski to Euclidean space. We define Euclidean time component as  $x_4^E = ix_0$ , spatial

coordinate components are not changed. The complete transition to Euclidean variables (denoted by the index E) requires the following relations: Vector potentials:

$$A_4^E = -iA_0, \quad A_i^E = -A_i \quad (i = 1, 2, 3). \quad (\text{A.1})$$

Covariant differentiation:

$$\nabla_4^E = -i\nabla_0, \quad \nabla_i^E = -\nabla_i \quad (i = 1, 2, 3) \quad (\text{A.2})$$

hence

$$\nabla_\mu^E = \frac{\partial}{\partial x_\mu^E} - igA_\mu^E. \quad (\text{A.3})$$

Stress tensor:

$$F_{\mu\nu}^{aE} = \frac{\partial}{\partial x_\mu^E} A_\nu^{aE} - \frac{\partial}{\partial x_\nu^E} A_\mu^{aE} + gf^{abc} A_\mu^{bE} A_\nu^{cE}. \quad (\text{A.4})$$

Gamma matrices:

$$\gamma_4^E = \gamma_0, \quad \gamma_i^E = -i\gamma_i \quad (i = 1, 2, 3) \quad (\text{A.5})$$

$$\{\gamma_\mu^E, \gamma_\nu^E\} = 2\delta_{\mu\nu}. \quad (\text{A.6})$$

Fermi fields:

$$\psi^E = \psi, \quad \bar{\psi}^E = i\bar{\psi}. \quad (\text{A.7})$$

Action:

$$\begin{aligned} W^E &= -iW \\ W &= \int d^4x \left( -\frac{1}{4} F_{\mu\nu}^a F_{\mu\nu}^a + \bar{\psi}(i\gamma_\mu \nabla_\mu - M)\psi \right) \\ W^E &= \int d^4x^E \left( \frac{1}{4} F_{\mu\nu}^{aE} F_{\mu\nu}^{aE} + \bar{\psi}^E (-i\gamma_\mu^E \nabla_\mu^E - iM)\psi^E \right). \end{aligned} \quad (\text{A.8})$$

Unless explicitly mentioned, all formulae in this paper are given in Euclidean space, therefore the index E is usually omitted.

### A.2. Zero modes and overlap integrals

We give the explicit form of the zero modes density matrices for the Instanton - Instanton case

$$\phi_I(x)_{i\alpha} \phi_{I'}^\dagger(y)_{j\beta} = \frac{1}{8} \varphi_I(x) \varphi_{I'}(y) \left( \not{x} \gamma_\mu \gamma_\nu \not{y} \frac{1 - \gamma_5}{2} \right)_{ij} \otimes (U_I \tau_\mu^- \tau_\nu^+ U_{I'})_{\alpha\beta}, \quad (\text{A.9})$$

Instanton — Anti-instanton case

$$\phi_I(x)_{i\alpha} \phi_I^\dagger(y)_{j\beta} = -i \frac{1}{8} \varphi_I(x) \varphi_I(y) \left( \not{x} \gamma_\mu \not{y} \frac{1 - \gamma_5}{2} \right)_{ij} \otimes (U_I \tau_\mu^- U_I^\dagger)_{\alpha\beta}, \quad (\text{A.10})$$

where

$$\varphi(x) = \frac{\rho_I}{\pi \sqrt{x^2} (x^2 + \rho_I^2)^{\frac{3}{2}}}. \quad (\text{A.11})$$

Overlap integrals are explicitly given by

$$\begin{aligned} D_{II} &\stackrel{\text{def}}{=} \int d^4x \phi_I^{\dagger i\alpha}(x - z_I) i \not{d} \phi^{i\alpha}(x - z) \\ &= \text{Tr}(U_I \tau_\mu^- U_I^\dagger) r_\mu \frac{1}{2\pi^2} \frac{1}{r} \frac{d}{dr} \mathcal{M}(r), \end{aligned} \quad (\text{A.12})$$

$$\begin{aligned} K_{II'} &\stackrel{\text{def}}{=} \int d^4x \phi_I^{\dagger i\alpha}(x - z_I) \phi_{I'}^{i\alpha}(x - z) - \delta_{II'} \\ &= \text{Tr}(U_I^\dagger U_{I'}) \frac{1}{2\pi^2} \mathcal{M}(r) - \delta_{II'} \end{aligned} \quad (\text{A.13})$$

where  $r_\mu = z_\mu^I - z_\mu^{I'}$ ,

$$\mathcal{M}(r) = \frac{1}{r} \int_0^\infty dp p^2 |\varphi(p)|^2 J_1(pr) \quad (\text{A.14})$$

and the Fourier transformations of the zero mode profile (A-11) is explicitly given by

$$\varphi(p) = \pi \rho^2 \frac{d}{dx} (I_0(x) K_0(x) - I_1(x) K_1(x)) \Big|_{x = \frac{|\rho|p}{2}}. \quad (\text{A.15})$$

## Appendix B

### *Group integration for the $SU(N_c)$ manifold*

Averaging over the color group requires the knowledge of the integrands over invariant measure of the following strings of the color matrices:

$$\underbrace{U_{i_1}^{a_1} U_{b_1}^{\dagger j_1}}_1 \dots \underbrace{U_{i_n}^{a_n} U_{b_n}^{\dagger j_n}}_{N_f}. \quad (\text{B.1})$$

Such string can be easily evaluated, using the observation that the group integration is equivalent to the projection of a tensor product of fundamental representations onto singlet of the group [74]. The case of one flavor (corresponding to the projection  $3 \otimes \bar{3} \rightarrow 1$ ) is particularly simple

$$\int dU U_i^a U_b^{\dagger j} = \frac{1}{N_c} \delta_b^a \delta_i^j. \quad (\text{B.2})$$

Two flavor case ( $3 \otimes \bar{3} \otimes 3 \otimes \bar{3} = (1 \oplus 8) \otimes (1 \oplus 8) \rightarrow 1$ ) requires two projections, the trivial one ( $1 \otimes 1 \rightarrow 1$ ) and octet-octet onto singlet projector  $8 \otimes 8 \rightarrow 1$ :

$$\begin{aligned} \int dU U_{i_1}^{a_1} U_{b_1}^{\dagger j_1} U_{i_2}^{a_2} U_{b_2}^{\dagger j_2} &= \frac{1}{N_c^2} \delta_{b_1}^{a_1} \delta_{j_1}^{i_1} \delta_{b_2}^{a_2} \delta_{j_2}^{i_2} \\ &+ \frac{1}{4(N_c^2 - 1)} [\lambda^i]_{b_1}^{a_1} [\lambda^i]_{b_2}^{a_2} [\lambda^j]_{i_1}^{j_1} [\lambda^j]_{i_2}^{j_2} \end{aligned} \quad (\text{B.3})$$

where the  $\lambda$ 's are the properly normalized generators of  $SU(N_c)$ . By using properties of the  $\lambda$ -matrices

$$[\lambda^i]_b^a [\lambda^i]_d^c = 2(\delta_d^a \delta_b^c - \frac{1}{N_c} \delta_b^a \delta_d^c) \quad (\text{B.4})$$

one can easily recover Creutz's standard result [75] for the  $SU(N_c)$  case.

In order to perform the group averaging in the three flavor case we need the following relation

$$\begin{aligned} \int dU U_{i_1}^{a_1} U_{b_1}^{\dagger j_1} U_{i_2}^{a_2} U_{b_2}^{\dagger j_2} U_{i_3}^{a_3} U_{b_3}^{\dagger j_3} &= \frac{1}{N_c^3} \delta_{b_1}^{a_1} \delta_{j_1}^{i_1} \delta_{b_2}^{a_2} \delta_{j_2}^{i_2} \delta_{b_3}^{a_3} \delta_{j_3}^{i_3} \\ &+ \frac{1}{4N_c(N_c^2 - 1)} \left( [\lambda^i]_{b_1}^{a_1} [\lambda^i]_{b_2}^{a_2} [\lambda^j]_{i_1}^{j_1} [\lambda^j]_{i_2}^{j_2} \delta_{b_3}^{a_3} \delta_{j_3}^{i_3} + (3 \leftrightarrow 1) + (2 \leftrightarrow 1) \right) \\ &+ \frac{N_c}{8(N_c^2 - 4)(N_c^2 - 1)} d_{ijk} d_{abc} [\lambda^i]_{b_1}^{a_1} [\lambda^j]_{b_2}^{a_2} [\lambda^k]_{b_3}^{a_3} [\lambda^a]_{j_1}^{i_1} [\lambda^b]_{j_2}^{i_2} [\lambda^c]_{j_3}^{i_3} \\ &+ \frac{1}{8N_c(N_c^2 - 1)} f_{ijk} f_{abc} [\lambda^i]_{b_1}^{a_1} [\lambda^j]_{b_2}^{a_2} [\lambda^k]_{b_3}^{a_3} [\lambda^a]_{j_1}^{i_1} [\lambda^b]_{j_2}^{i_2} [\lambda^c]_{j_3}^{i_3}. \end{aligned} \quad (\text{B.5})$$

In this case we project  $3 \otimes \bar{3} \otimes 3 \otimes \bar{3} \otimes 3 \otimes \bar{3} = (1 \oplus 8) \otimes (1 \oplus 8) \otimes (1 \oplus 8) \rightarrow 1$ . The first term in the above formula corresponds to a trivial projection  $1 \otimes 1 \otimes 1$ , the second line corresponds to the three projections of the two octets onto the singlet ( $1 \otimes 8 \otimes 8 \rightarrow 1$  or  $8 \otimes 1 \otimes 8 \rightarrow 1$  or  $8 \otimes 8 \otimes 1 \rightarrow 1$ ) and the last two lines correspond to the two kinds of projections (involving symmetric and antisymmetric octets) of the three octets ( $8 \otimes 8 \otimes 8$ ) onto the singlet. With the help of the decomposition (B-4) and the following relations

$$\frac{i}{2} f_{ijk} [\lambda^i]_a^b [\lambda^j]_c^d [\lambda^k]_e^f = \delta_a^d \delta_e^b \delta_c^f - \delta_a^f \delta_c^b \delta_e^d, \quad (\text{B.6})$$

$$\begin{aligned} \frac{1}{2} d_{ijk} [\lambda^i]_a^b [\lambda^j]_c^d [\lambda^k]_e^f &= \delta_a^f \delta_e^d \delta_c^b + \delta_c^f \delta_e^b \delta_a^d + \frac{4}{N_c} \delta_e^f \delta_c^d \delta_a^b \\ &\quad - \frac{2}{N_c} (\delta_a^f \delta_e^b \delta_c^d + \delta_e^d \delta_c^f \delta_a^b + \delta_e^f \delta_a^d \delta_c^b) \end{aligned} \quad (\text{B.7})$$

we can rewrite this result in products of the Kronecker deltas. Results for  $SU(2)$  can be obtained by skipping terms involving  $d_{ijk}$  and by setting  $f_{ijk} = \varepsilon_{ijk}$ . Note, that the leading in  $N_c$  terms are the products of  $N_f$  terms of the one flavor case. This large  $N_c$  behaviour, accompanied by the properties of the invariant measure, guarantees that the ensemble of the instantons behaves like the Gaussian orthogonal ensemble in the limit  $N_c \rightarrow \infty$ .

**Note added in proof:** After completion of this manuscript two papers, addressing the problem of the “best” ansatz, were brought to our attention. In the first one [76], the numerical solution of the instanton-anti-instanton pair configuration was presented. The solution resembles surprisingly the ansatz proposed some time ago in [77] by imposing the conformal invariance. In the second one [78], an ansatz-independent description of the instanton vacuum was suggested on the basis of the unitarity principle. Further investigation in this direction looks very promising. New results have been also obtained for the finite temperature case. The crucial role of the fermionic correlations was explicitly confirmed by the finite temperature numerical simulation done in [79].

## REFERENCES

- [1] E.M. Shuryak, *The QCD vacuum, hadrons and the superdense matter*, World Scientific, 1987.
- [2] For a review see L. Reinders, H. Rubinstein, S. Yazaki, *Phys. Rep.* **127**, 1 (1985).
- [3] G.K. Savvidy, *Phys. Lett.* **71B**, 133 (1982).
- [4] N.K. Nielsen, P. Olesen, *Nucl. Phys.* **B144**, 376 (1978).
- [5] G. 't Hooft, *Phys. Scr.* **25**, 133 (1982).
- [6] T.H. Hansson, K. Johnson, C. Peterson, *Phys. Rev.* **D26**, 2069 (1982).
- [7] C.G. Callan, R. Dashen, D.J. Gross, *Phys. Rev.* **D17**, 2717 (1978).
- [8] V.A. Novikov, M.A. Shifman, A.I. Vainshtein, V.I. Zakharov, *Nucl. Phys.* **B191**, 301 (1981).
- [9] J. Greensite, *Nucl. Phys.* **B249**, 263 (1985).
- [10] Yu. A. Simonov, *Yad.Fiz.* **50**, 500 (1989).
- [11] C. DeTar, *Phys.Rev.* **D32**, 276 (1985).
- [12] T.A. DeGrand, C.E. DeTar, *Is the quark-gluon plasma dynamically confined?*, in: *Workshop on Nuclear Chromodynamics: Quarks and Gluons in Particles*

and Nuclei, Santa Barbara, California 1985, eds: S. Brodsky E. Moniz, World Scientific, 1986.

- [13] G. 't Hooft, *Phys.Rev.* **D14**, 3432 (1976).
- [14] M.A. Shifman, A.I. Vainshtein, V.I. Zakharov, *Phys.Lett.* **76B**, 971 (1978).
- [15] C.G. Callan, R.F. Dashen, D.J. Gross, *Phys. Rev.* **D17**, 2717 (1978).
- [16] R.D. Carlitz, *Phys.Rev.* **D17**, 3225 (1978).
- [17] D.I. Diakonov, V.Yu. Petrov, *Nucl. Phys.* **B245**, 259 (1984).
- [18] D.I. Diakonov, V.Yu. Petrov, *Nucl. Phys.* **B272**, 457 (1986).
- [19] E.V. Shuryak, *Phys. Lett.* **193B**, 319 (1987).
- [20] E.V. Shuryak, *Nucl. Phys.* **B302**, 599 (1988).
- [21] E.V. Shuryak, *Nucl. Phys.* **B319**, 521 (1989).
- [22] M.A. Nowak, J.J.M. Verbaarschot, I. Zahed, *Nucl. Phys.* **B324**, 1 (1989).
- [23] J.J.M. Verbaarschot, E.V. Shuryak, *Nucl. Phys.* **B341**, 1 (1990).
- [24] M.A. Nowak, J.J.M. Verbaarschot, I. Zahed, *Nucl. Phys.* **B335**, 1 (1989).
- [25] M.A. Nowak, J.J.M. Verbaarschot, I. Zahed, *Phys. Lett.* **217B**, 157 (1989).
- [26] M.A. Nowak, J.J.M. Verbaarschot, I. Zahed, *Phys. Lett.* **228B**, 115 (1989).
- [27] R. Alkofer, M.A. Nowak, J.J.M. Verbaarschot, I. Zahed, *Phys. Lett.* **233B**, 205 (1989).
- [28] A.A. Belavin, A.M. Polyakov, A.A. Schwartz, Yu.S. Tyupkin, *Phys.Lett.* **59B**, 85 (1975).
- [29] R. Rajaraman, *Solitons and instantons*, North Holland, 1982.
- [30] A.M. Polyakov, *Gauge fields and strings*, Harwood Academic Publ., 1987.
- [31] E.V. Shuryak, *Nucl. Phys.* **B302**, 574 (1988).
- [32] E.V. Shuryak, *Physics Rep.* **115**, 151 (1984).
- [33] A.I. Vainshtein, V.I. Zakharov, V.A. Novikov, M.A. Shifman, *Nucl. Phys.* **B191**, 301 (1981).
- [34] E.V. Shuryak, *Nucl. Phys.* **B297**, 47 (1988).
- [35] J.J.M. Verbaarschot, private communication.
- [36] E.V. Shuryak, *Nucl. Phys.* **B302**, 559 (1988).
- [37] J.M. Ziman, *Models of disorder*, Cambridge University Press, 1979.
- [38] T.H. Hansson, M. Prakash, I. Zahed, Stony Brook preprint, October 1987.
- [39] O. Bohigas, M.J. Giannoni, C. Schmit, *Phys.Rev.Lett.* **52**, 1 (1984).
- [40] T.H. Seligman, J.J.M. Verbaarschot, M.R. Zirnbauer, *Phys.Rev.Lett.* **53**, 215 (1984).
- [41] F.J. Dyson, *Comm.Math.Phys.* **19**, 235 (1970).
- [42] M.L. Mehta, *Comm.Math.Phys.* **20**, 245 (1971).
- [43] D.I. Diakonov, V.Yu. Petrov, Leningrad Preprint LNPI-1153, 1986.
- [44] N. Andrei, D.J. Gross, *Phys. Rev.* **18D**, 468 (1978).
- [45] E.M. Ilgenfritz, Habilitation Leipzig, 1988.
- [46] M.A. Shifman, A.I. Vainshtein, V.I. Zakharov, *Nucl. Phys.* **B163**, 43 (1980).
- [47] D.I. Diakonov, private communication.
- [48] J. Engels, F. Karsch, I. Montvay, H. Satz, *Nucl. Phys.* **B205**, 545 (1982).
- [49] J. Kuti, J. Polonyi, K. Szlachnyi, *Phys.Lett.* **98B**, 199 (1981).
- [50] D.G. Caldi, *Phys. Rev. Lett.* **39**, 121 (1977).
- [51] T. Kanki, Osaka University Preprint OSGE 86-24, 1988.

- [52] D.I. Diakonov, A.D. Mirlin, *Phys. Lett.* **203B**, 299 (1988).
- [53] E.M. Ilgenfritz, E.V. Shuryak, *Nucl. Phys.* **B203**, 140 (1982).
- [54] B.J. Harrington, H.K. Shepard, *Phys. Rev.* **D17**, 2122 (1978).
- [55] D.J. Gross, R.D. Pisarski, L.G. Yaffe, *Rev. Mod. Phys.* **53**, 43 (1981).
- [56] D.I. Diakonov, V.Yu. Petrov, *Sov. Phys. JETP* **89**, 361 (1985).
- [57] P. Di Vecchia, *Phys. Lett.* **85B**, 357 (1979).
- [58] J. Schechter, *Phys. Rev.* **D21**, 3394 (1980).
- [59] G. Veneziano, *Nucl. Phys.* **B159**, 461 (1979).
- [60] E. Witten, *Nucl. Phys.* **B156**, 269 (1979).
- [61] F.J. Gillman, R. Kauffman, *Phys. Rev.* **D36**, 2761 (1987).
- [62] Yu.A. Simonov, Minnesota preprint TPI-MINN 90/30-T.
- [63] S.J. Hands, M. Teper, *Nucl. Phys.* **B347**, 819 (1990).
- [64] J. Kogut, D. Sinclair, M. Teper, *Nucl. Phys.* **B348**, 178 (1991).
- [65] N.H. Christ, Columbia preprint CU-TP-504.
- [66] F. Karsch, CERN preprint TH-5498/89.
- [67] R.D. Pisarski, F. Wilczek, *Phys. Rev.* **D29**, 338 (1984).
- [68] Y. Nambu, G. Jona-Lasinio, *Phys. Rev.* **122**, 345 (1961).
- [69] P.V. Pobylitsa, *Phys. Lett.* **226B**, 387 (1989).
- [70] E.V. Shuryak, *Nucl. Phys.* **B328**, 102 (1989).
- [71] E.V. Shuryak, *Nucl. Phys.* **B328**, 85 (1989).
- [72] M.A. Nowak, J.J.M. Verbaarschot, I. Zahed, *Phys. Lett.* **226B**, 382 (1989).
- [73] S. Forte, E.M. Shuryak, CEN Saclay preprint SPhT/90-159.
- [74] P. Cvitanovic, *Group Theory*, Nordita Notes, 1984.
- [75] M. Creutz, *J. Math. Phys.* **19**, 2043 (1978).
- [76] J.J.M. Verbaarschot, Stony Brook preprint, SUNY-NTG-91/7 (1991).
- [77] A.V. Yung, *Nucl. Phys.* **B297**, 47 (1988).
- [78] D.I. Diakonov, V.Yu. Petrov, talk at XXXI Cracow School of Theoretical Physics, Zakopane 1991.
- [79] E.V. Shuryak, J.J.M. Verbaarschot, Stony Brook preprint, SUNY-NTG-91/3 (1991).